ternal ribosomal entry site (IRES) sequence was amplified by polymerase chain reaction (PCR) on the encephalomyocarditis virus genome (nucleotides 259–833), using primers A (5′-GCATTCCTAGGGGTCTTTCC-3′) and B (5′-CCATCTTGTTCAATCATATTATCATCGTGTTTTTCAA-3′).[9,10] The neomycin phosphotransferase gene (neo) was derived from pRSVneo by PCR with primers C (5′-TTGAAAAACACGATGATAATATGATTGAACAAGATGG-3′) and D (5′-CCGACTCGAGTCAGAAGAACTCGTC-3′).[11] Primers B and C were designed to create an overlap between the 3′-end of the IRES and the 5′-end of the neo PCR products, and the IRESneo fragment was PCR-amplified on them with primers A and D. The MfasER and IRESneo fragments were cloned into pMX retroviral vector (a gift from Dr. T. Kitamura, University of Tokyo, Tokyo).[12] The resultant bicistronic retroviral vector was designated pMX/MfasER-IRESneo. In order to increase the expression, a CAG promoter sequence (a gift from Dr. J. Miyazaki, Osaka University, Osaka; Ref. 13) was inserted into pMX/MfasER-IRESneo, at the site between the 5′-long terminal repeat (LTR) and MfasER gene. The resultant vector was designated pMX/CAGMfasER-IRESneo.

Cell culture and transfection. CTLL-2, a murine cytotoxic T cell line (a gift from Dr. K. Sugamura, Tohoku University, Sendai),[8] was maintained in RPMI-1640 medium supplemented with 10% fetal bovine serum (FBS; Sigma, St. Louis, MO), 10 U/ml of recombinant human interleukin-2 (IL-2) (Imunace; provided by Shionogi, Osaka), 2 m*M* L-glutamine (Invitrogen, Grand Island, NY) and 50 μM 2-mercaptoethanol. The expression plasmid, pMX/CAGMfasER-IRESneo, was linearized between the 5′-LTR and CAG promoter sequence and electroporated into CTLL-2 cells using a Gene Pulser (Bio-Rad, Hercules, CA). Stably transfected cells were selected by culturing in medium supplemented with 1.0 mg/ml of G418 (Invitrogen). We designated the final cell population as CTLL/MfasER. RLmale1 mouse T cell leukemia line was maintained in RPMI-1640 with 10% FBS.[14]

Induction of growth inhibition and apoptosis. To assess estrogen-dependent apoptosis, CTLL/MfasER cells and parental CTLL-2 cells were harvested from standard cultures, and recultured at an initial density of 5×10^4 cells/ml in medium with 10^{-7} *M* 17β-estradiol (E_2) (Sigma) or 0.05% ethanol (solvent for E_2). After designated periods of incubation, CTLL/MfasER and CTLL-2 cells were examined on an inverted microscope (IX-70; Olympus, Tokyo). Viable cells were counted by the trypan blue exclusion method and photographed (original magnification, 500×). The number of viable cells at each time point was standardized with the value for 0 h taken as 100%. Cytospin preparations were also made for morphological examination.

Cell-mediated cytotoxicity assays. To determine CTL activities of CTLL-2 cells, a standard ^{51}Cr release assay was performed as described,[15] using RLmale1 cells as the target. Briefly, CTLL-2 and MfasER/CTLL effector cells were deprived of IL-2 in the presence or absence of 10^{-7} *M* E_2. After 12 h, the effector cells were stimulated with 20 U/ml of IL-2 for 2 h. Meanwhile, 1×10^6 RLmale1 cells were radiolabeled with 50 μCi of $Na_2{}^{51}CrO_4$ for 2 h at 37°C, washed three times with phosphate-buffered saline (PBS) and resuspended in the culture medium at 1×10^5 cells/ml. The radiolabeled target cells were inoculated onto 96-well round-bottomed microtiter plates (1×10^4 cells in 0.1 ml per well), to which serially diluted effector cells were added. The mixed cells were incubated in a total volume of 0.2 ml for 4 h at 37°C. The ^{51}Cr released into the supernatant was measured with a γ-scintillation counter (ARC-300; Aloka, Tokyo) and designated experimental release (R_{ex}). In parallel, spontaneous release (R_{sp}) was determined by the incubation of target cells without effector cells, and maximal release (R_{max}) was obtained by lysing 1×10^4 target cells in 1% Triton X-100. The percent specific lysis was calculated from the following formula:

$$\%\ \text{specific lysis}=[(R_{ex}-R_{sp})/(R_{max}-R_{sp})]\times100.$$

The cytotoxicity assay was performed in triplicate, with varying effector/target (E/T) ratios.

Western blot analysis. CTLL-2 and CTLL/MfasER cells were harvested and washed three times with PBS. The cells were lysed with Triton X-100 buffer [1% Triton X-100, 50 m*M* Tris-HCl (pH 7.4), 150 m*M* NaCl, 100 m*M* EGTA, 1.5 m*M* $MgCl_2$ and a protease inhibitor cocktail tablet (Complete Mini; Roche Diagnostics, Mannheim, Germany)] for 60 min on ice. After centrifugation, cell lysates (from 2.5×10^6 cells for each sample, counted at the beginning of E_2 exposure) were heated at 100°C for 5 min in Laemmli's sample buffer [62.5 m*M* Tris-HCl (pH 6.8), 2% sodium dodecyl sulfate (SDS), 10% glycerol and 5% 2-mercaptoethanol] and subjected to SDS-10% polyacrylamide gel electrophoresis. Subsequently, the proteins were electroblotted onto polyvinylidene fluoride membrane (Immobilon-P; Millipore, Yonezawa). The membrane was blocked with 5% bovine serum albumin (Roche Diagnostics), then incubated with a rat anti-mouse perforin antibody (KM585; Kamiya Biomedical, Seattle, WA) or a rabbit anti-rat FasL antibody (C-178; Santa Cruz Biotechnology, Santa Cruz, CA). Horseradish peroxidase-conjugated rabbit anti-rat IgG or goat anti-rabbit IgG, respectively, was used as a secondary antibody and the signal was visualized with an ECL detection kit (Amersham Pharmacia Biotech, Piscataway, NJ).

Results

Establishment of CTLL-2 cells expressing MfasER fusion protein. The structure of MfasER is illustrated in Fig. 1. MfasER is a chimeric protein made of the transmembrane through cytoplasmic portion of the mouse Fas (amino acids 135–305) and the carboxyl-half of the rat ER (amino acids 286–600).[16,17] The intracellular region of Fas contains a "death domain" of about 70 amino acids, which plays an essential role in apoptotic signal transduction.[18] The transmembrane domain of Fas was required for the fusion protein to anchor to the membrane and transmit a death signal.[4] The carboxyl-half of the ER contains the LBD and a ligand-induced dimerization motif,[19] which activates the chimeric receptor in an estrogen-dependent manner. CTLL-2 cells were transfected with the plasmid pMX/CAGMfasER-IRESneo, then subjected to G418 selection to produce stable cells expressing MfasER. The established line was designated CTLL/MfasER.

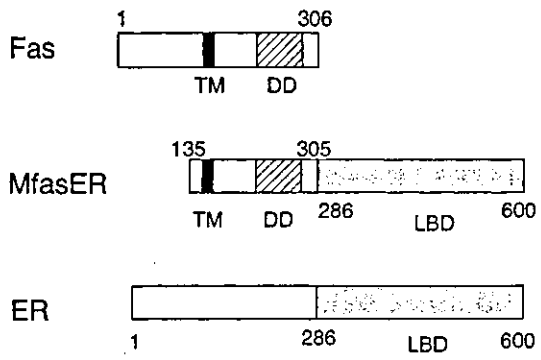

Fig. 1. Schematic structures of mouse Fas (top), rat estrogen receptor (ER; bottom), and MfasER fusion protein (middle; Ref. 4). The amino acid numbers of the original Fas and ER are shown above and below the schematics, respectively. TM (closed box), transmembrane region of Fas (amino acids 149–165); DD (hatched box), death domain of Fas (amino acids 201–286); LBD (shaded box), ligand-binding domain of ER (amino acids 286–600).

Estrogen-induced cell death of CTLL/MfasER. Without estrogen in the culture medium, both CTLL-2 and CTLL/MfasER cells showed IL-2-dependent growth. Although CTLL/MfasER cells proliferated at a slightly slower rate than the parental cells, the transfected cells exhibited continuous growth in the maintenance medium. While the addition of 10^{-7} *M* E_2 had no effect on the growth of parental CTLL-2 cells (Fig. 2A), the same dose of E_2 inhibited the growth of CTLL/MfasER cells nearly completely (Fig. 2B). Addition of the vehicle (0.05% ethanol) did not affect the proliferation of CTLL-2 or CTLL/MfasER cells (Fig. 2, A and B), compared with the cells in the maintenance medium (not shown).

The growth inhibition of CTLL/MfasER by estrogen was closely associated with the selective induction of apoptosis in these cells. Exposure to 10^{-7} *M* E_2 caused the shrinkage of CTLL/MfasER cells, with nuclear condensation and fragmentation. Finally, 80–90% of the cells were killed in 36 h (Fig. 2D). On the other hand, this concentration of E_2 did not affect the parental CTLL-2 cells (Fig. 2C). Similarly, the viabilities of CTLL-2 and CTLL/MfasER cells in 0.05% ethanol-containing medium were ~100% (Fig. 2, C and D). Fig. 3 shows the morphology of CTLL/MfasER cells treated with E_2. The cells were exposed to E_2 for the period of time indicated, and observed with a microscope using the trypan blue exclusion method (original magnification, 500×). Almost all of the treated CTLL/MfasER cells were shrunk and stained blue, having undergone the process of apoptosis, similarly to MfasER-expressing L929 fibroblasts upon E_2 treatment.[4,5]

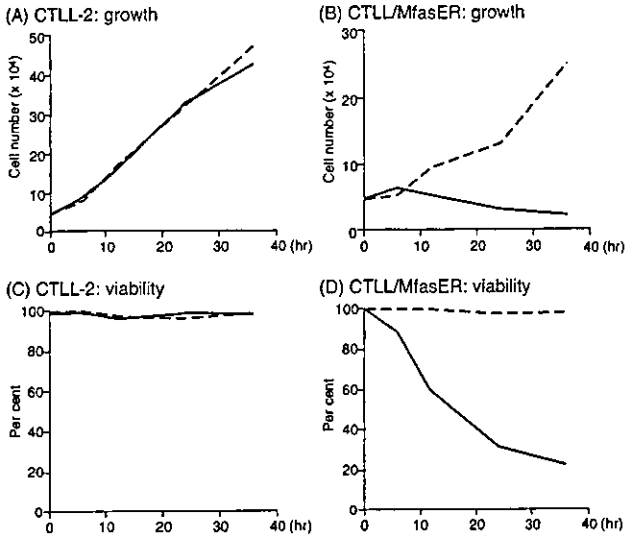

Fig. 2. Estrogen response to parental and MfasER-transduced CTLL-2 cells. The left column represents the growth (A) and viability (C) of parental CTLL-2, and the right column represents the growth (B) and viability (D) of CTLL/MfasER. Cells were cultured in IL-2-containing RPMI medium, either with 10^{-7} *M* 17β-estradiol (E_2; solid line) or vehicle (0.05% ethanol; broken line).

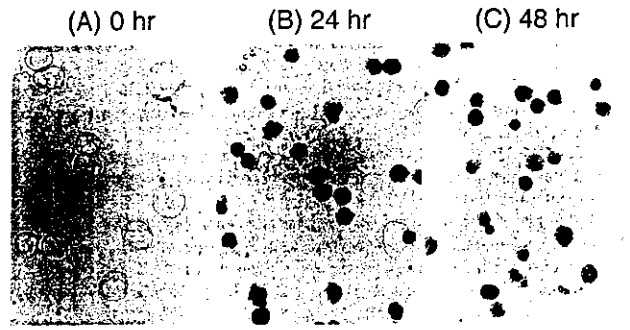

Fig. 3. Cytospin preparation of MfasER/CTLL cells stained with trypan blue dye. Cells were photographed at 0 h (A), 24 h (B), and 48 h (C) after addition of 10^{-7} *M* E_2 (original magnification, 500×). Viability decreased from ~100% to 30% in 24 h, and to <20% in 48 h.

Inhibition of CTLL/MfasER cytotoxicity by estrogen. Crucial to the clinical application of CTLs for apoptosis induction is whether the suicide system rapidly terminates an aggressive killing event. Thus, we examined the cytotoxic activity of CTLL/MfasER cells in the absence and presence of estrogen, by means of a standard ^{51}Cr release assay. In our preliminary study, RLmale1, a radiation-induced mouse T cell leukemia line,[14] was the most appropriate target among several candidates (data not shown). Therefore we used RLmale1 as the target in the subsequent experiments.

As shown in Fig. 4A, the parent CTLL-2 cells killed up to 55% of RLmale1 cells either in the absence or presence of E_2, and the cytotoxic activity was dependent on the E/T ratio. In the absence of E_2, CTLL/MfasER cells showed an even greater cytotoxicity than the parental cells (up to 90% killing at an E/T ratio of 10; Fig. 4B, broken line). However, addition of 10^{-7} *M* E_2 dramatically reduced their killing activity. After 14 h of exposure to E_2, CTLL/MfasER showed very little cytotoxicity (up to 20% killing; Fig. 4B, solid line). These results clearly indicated that MfasER expression *per se* did not impair killing activity in CTLL-2 cells, and that the cytotoxicity was dramatically inhibited when the chimeric protein was activated by es-

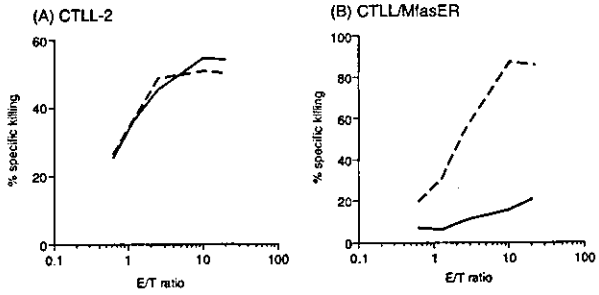

Fig. 4. ^{51}Cr release assay for cytotoxic activity of CTLL/MfasER cells. Ten thousand ^{51}Cr-labeled RLmale1 cells were plated in 96-well microtiter plates as the target. CTLL/MfasER cells were treated with 10^{-7} *M* E_2 or 0.05% ethanol (vehicle) for 14 h, then added to ^{51}Cr-labeled RLmale1 at the indicated effector/target (E/T) ratios. After 4 h of incubation, ^{51}Cr released into the supernatant was measured, and the percent specific lysis was determined as described in "Materials and Methods." Solid lines indicate specific killing by E_2-treated CTLL/MfasER, and broken lines represent specific killing by vehicle-treated cells.

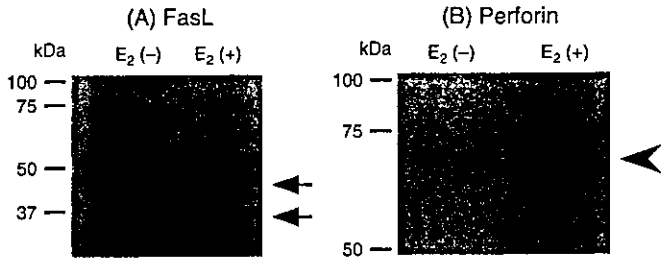

Fig. 5. Expression of Fas ligand (FasL) and perforin in E_2-treated CTLL/MfasER. Two and a half million CTLL/MfasER cells were treated with 10^{-7} *M* E_2 or 0.05% ethanol (vehicle) for 12 h. Cell lysate was electrophoresed and blotted, and the membranes were hybridized with an anti-FasL (A) or an anti-perforin (B) antibody. E_2(–), vehicle-treated CTLL/MfasER; E_2(+), E_2-treated CTLL/MfasER. Arrows indicate FasL (35 kDa and 50 kDa), and arrowhead indicates perforin (69 kDa).

trogen. Therefore, MfasER-expressing CTLs would effectively eliminate allogeneic target cells, and themselves be rapidly eradicated by estrogen when necessary.

Diminished expression of apoptosis-related proteins in estrogen-treated CTLL/MfasER. When cytotoxic T cells exert cytotoxicity, they induce apoptosis in the target cells mainly via FasL and perforin/granzyme pathways.[20-22] We investigated whether levels of these effector proteins such as FasL and perforin were also decreased upon estrogen treatment. The expression levels of FasL and perforin in CTLL/MfasER cells before and after estrogen treatment were examined by western blot analysis (Fig. 5). Without E_2, CTLL/MfasER cells contained 35 kDa and 50 kDa proteins detectable with an anti-FasL antibody (Fig. 5A, left lane). The predicted molecular weight of mouse FasL is 31 kDa, with four potential N-glycosylation sites in its extracellular domain, and several studies have shown that the apparent molecular weight of FasL in different cell lines varies from 36 to 43 kDa.[23] Therefore we considered that the 35 kDa species was the unmodified FasL and the 50 kDa protein was a glycosylated form of FasL. After 12 h of E_2 exposure, these bands were diminished in CTLL/MfasER, concomitantly with apoptosis induction in these cells (Fig. 5A, right lane). Furthermore, we obtained a similar result for perforin expression. While perforin was detected as a 69 kDa protein in the untreated CTLL/MfasER (Fig. 5B, left lane), this band was almost undetectable in the E_2-treated cells (Fig. 5B, right lane).

Discussion

Suicide gene therapy has been explored in several anti-cancer strategies. Such approaches include the direct killing of neoplastic cells, eradication of donor lymphocytes responsible for severe GVHD, and elimination of cytokine producer cells to terminate supplementary gene therapy. So far, most of the "suicide vectors" have incorporated the HSVtk gene, and several clinical studies have been performed, including some on DLI after allogeneic BMT.[2,3] In the present study, we used the MfasER/estrogen system as an alternative to the HSVtk/GCV system. We introduced the MfasER gene into the mouse CTL line CTLL-2 and evaluated the effectiveness of estrogen treatment in inducing apoptosis. MfasER induced rapid and extensive cell death in the transduced cells, accompanied with a massive reduction in cytotoxic activity. These results implied that the use of the MfasER/estrogen system is feasible for controlling CTLs involved in GVHD following DLI.

One of the concerns with the MfasER/estrogen system is that endogenous estrogen might constitutively activate ER-containing fusion molecules. It has been reported that 10^{-10} M or more of E_2 was required to induce apoptosis in MfasER-transduced L929 cells, a concentration considerably exceeding the physiological level of blood estrogen in female mice.[4] When transplanted into nude mice, the MfasER-expressing cells proliferated without interference from endogenous steroids, and the cells showed an apoptotic phenotype only when estrogen was administered exogenously. Thus, engineered cells similar to CTLL/MfasER are expected to survive and exert cytotoxic activity in the recipient animals, but to be eliminated by E_2 administration.

Still, it is desirable to minimize unwanted apoptosis in genetically modified cells, which may be induced by elevated levels of estrogen in females.[24] In addition, the administration of estrogen may be associated with adverse effects such as coagulopathy. One strategy to overcome these concerns is to use a mutant ER with an altered specificity. For example, a mutant receptor (TmR), with an arginine substitution for glycine 525, is unresponsive to estrogen and responds specifically to a synthetic estrogen analog, 4-hydroxytamoxifen (Tm).[25] A Fas fusion protein with TmR (MfasTmR) converted L929 cells to a Tm-induced apoptotic phenotype.[10] The pharmacological profile of tamoxifen has been well characterized through its usage as a therapeutic drug, which may be an advantage in considering the MfasTmR/tamoxifen system as a candidate clinical tool to induce apoptosis in patients. Thomis *et al.* employed yet another molecular switch to activate Fas. They fused multiple copies of FK506-binding motifs to Fas, and used a dimeric compound, AP1903, to crosslink the fusion protein.[26] Administration of AP1903 induced a rapid and extensive apoptosis in the transduced primary human T cells, regardless of the cell cycle status.

The effectiveness of Fas fusion proteins raises the possibility that other apoptosis-mediating molecules may also be incorporated in this system. For example, the recruitment of downstream molecules such as FADD/MORT1, TRAIL and caspase 9 might be considered in suicide gene therapy for CTLs.[27] Such investigations could increase the efficacy of this approach, and broaden the range of clinical applications. In any case, a better understanding of the alloreactive immune response and the identification of effector cells responsible for GVL and GVHD is required. If we can target more restricted cell populations, more sophisticated means for the control of GVHD can be explored.

We are grateful to Dr. A. Kakizuka (Kyoto University, Kyoto) for MfasER, Dr. T. Kitamura (University of Tokyo, Tokyo) for pMX, Dr. J. Miyazaki (Osaka University, Osaka) for CAG promoter and Dr. K. Sugamura (Tohoku University, Sendai) for CTLL-2. We also thank Shionogi Co., Ltd. (Osaka) for IL-2. This work was supported in part by Grants-in-Aid from the Ministry of Health, Labour and Welfare, the Ministry of Education, Culture, Sports, Science and Technology, and the Mochida Memorial Foundation for Medical and Pharmaceutical Research. M. K. was the recipient of a Research Award to Jichi Medical School Graduate Students.

1. Barrett AJ. Mechanisms of the graft-versus-leukemia reaction. *Stem Cells* 1997; **15**: 248–58.
2. Bonini C, Ferrari G, Verzeletti S, Servida P, Zappone E, Ruggieri L, Ponzoni M, Rossini S, Mavilio F, Traversari C, Bordignon C. HSV-TK gene transfer into donor lymphocytes for control of allogeneic graft-versus-leukemia. *Science* 1997; **276**: 1719–24.
3. Verzeletti S, Bonini C, Marktel S, Nobili N, Ciceri F, Traversari C, Bordignon C. Herpes simplex virus thymidine kinase gene transfer for controlled graft-versus-host disease and graft-versus-leukemia: clinical follow-up and improved new vectors. *Hum Gene Ther* 1998; **9**: 2243–51.
4. Takebayashi H, Oida H, Fujisawa K, Yamaguchi M, Hikida T, Fukumoto M, Narumiya S, Kakizuka A. Hormone-induced apoptosis by Fas-nuclear receptor fusion proteins: novel biological tools for controlling apoptosis *in vivo*. *Cancer Res* 1996; **56**: 4164–70.
5. Kokubun M, Kume A, Urabe M, Mano H, Okubo M, Kasukawa R, Kakizuka A, Ozawa K. Apoptosis-mediated regulation of recombinant human granulocyte colony-stimulating factor production by genetically engineered fibroblasts. *Gene Ther* 1998; **5**: 923–9.
6. Mattioni T, Louvion J-F, Picard D. Regulation of protein activities by fusion to steroid binding domains. *Methods Cell Biol* 1994; **43**: 335–52.
7. Nagata S, Golstein P. The Fas death factor. *Science* 1995; **267**: 1449–56.
8. Gillis S, Smith KA. Long term culture of tumour-specific cytotoxic T cells. *Nature* 1977; **268**: 154–6.
9. Duke GM, Hoffman MA, Palmenberg AC. Sequence and structural elements that contribute to efficient encephalomyocarditis virus RNA translation. *J Virol* 1992; **66**: 1602–9.
10. Kodaira H, Kume A, Ogasawara Y, Urabe M, Kitano K, Kakizuka A, Ozawa K. Fas and mutant estrogen receptor chimeric gene: a novel suicide vector for tamoxifen-inducible apoptosis. *Jpn J Cancer Res* 1998; **89**: 741–7.
11. Gorman C, Padmanabhan R, Howard BH. High efficiency DNA-mediated transformation of primate cells. *Science* 1983; **221**: 551–3.
12. Onishi M, Kinoshita S, Morikawa Y, Shibuya A, Phillips J, Lanier LL, Gorman DM, Nolan GP, Miyajima A, Kitamura T. Applications of retrovirus-mediated expression cloning. *Exp Hematol* 1996; **24**: 324–9.
13. Niwa H, Yamamura K, Miyazaki J. Efficient selection for high-expression transfectants with a novel eukaryotic vector. *Gene* 1991; **108**: 193–200.

14. Nakayama E, Shiku H, Takahashi T, Oettgen HF, Old LJ. Definition of a unique cell surface antigen of mouse leukemia RL male 1 by cell-mediated cytotoxicity. *Proc Natl Acad Sci USA* 1979; **76**: 3486–90.
15. Grabstein K, Chen YU. Cell-mediated cytolytic responses. In: Mishell BB, Shiigi SM, editors. Selected methods in cellular immunology. San Francisco: WH Freeman; 1980. p. 124–37.
16. Watanabe-Fukunaga R, Brannan CI, Itoh N, Yonehara S, Copeland NG, Jenkins NA, Nagata S. The cDNA structure, expression, and chromosomal assignment of the mouse Fas antigen. *J Immunol* 1992; **148**: 1274–9.
17. Koike S, Sakai M, Muramatsu M. Molecular cloning and characterization of rat estrogen receptor cDNA. *Nucleic Acids Res* 1987; **15**: 2499–513.
18. Itoh N, Nagata S. A novel protein domain required for apoptosis. *J Biol Chem* 1993; **268**: 10932–7.
19. Kumar V, Chambon P. The estrogen receptor binds tightly to its responsive element as a ligand-induced homodimer. *Cell* 1988; **55**: 145–56.
20. Braun MY, Lowin B, French L, Acha-Orbea H, Tschopp J. Cytotoxic T cells deficient in both functional Fas ligand and perforin show residual cytolytic activity yet lose their capacity to induce lethal acute graft-versus-host disease. *J Exp Med* 1996; **183**: 657–61.
21. Baker MB, Riley RL, Podack ER, Levy RB. Graft-versus-host-disease-associated lymphoid hypoplasia and B cell dysfunction is dependent upon donor T cell-mediated Fas-ligand function, but not perforin function. *Proc Natl Acad Sci USA* 1997; **94**: 1366–71.
22. Schmaltz C, Alpdogan O, Horndasch KJ, Muriglan SJ, Kappel BJ, Teshima T, Ferrara JLM, Burakoff SJ, van den Brink MRM. Differential use of Fas ligand and perforin cytotoxic pathways by donor T cells in graft-versus-host disease and graft-versus-leukemia effect. *Blood* 2001; **97**: 2886–95.
23. Suda T, Takahashi T, Golstein P, Nagata S. Molecular cloning and expression of the Fas ligand, a novel member of the tumor necrosis factor family. *Cell* 1993; **75**: 1169–78.
24. Ushiroyama T, Sugimoto O. Endocrine function of the peri- and postmenopausal ovary. *Horm Res* 1995; **44**: 64–8.
25. Littlewood TD, Hancock DC, Danielian PS, Parker MG, Evan GI. A modified oestrogen receptor ligand-binding domain as an improved switch for the regulation of heterologous proteins. *Nucleic Acids Res* 1995; **23**: 1686–90.
26. Thomis DC, Marktel S, Bonini C, Traversari C, Gilman M, Bordignon C, Clackson T. A Fas-based suicide switch in human T cells for the treatment of graft-versus-host disease. *Blood* 2001; **97**: 1249–57.
27. Fan L, Freeman KW, Khan T, Pham E, Spencer DM. Improved artificial death switches based on caspases and FADD. *Hum Gene Ther* 1999; **10**: 2273–85.

THE JOURNAL OF GENE MEDICINE
J Gene Med 2003; 5: 438–445.
Published online 23 December 2002 in Wiley InterScience (www.interscience.wiley.com). DOI: 10.1002/jgm.356

RESEARCH ARTICLE

A DNA vaccine containing inverted terminal repeats from adeno-associated virus increases immunity to HIV

Ke-Qin Xin[1]
Takaaki Ooki[1]
Nao Jounai[1]
Hiroaki Mizukami[2]
Kenji Hamajima[1]
Yoshitsugu Kojima[1]
Kenji Ohba[1]
Yoshihiko Toda[1]
Syu-Ichi Hirai[3]
Dennis M. Klinman[4]
Keiya Ozawa[2]
Kenji Okuda[1]*

[1]*Department of Bacteriology, Yokohama City University School of Medicine, Yokohama 236-0004, Japan*

[2]*Division of Genetic Therapeutics, Center for Molecular Medicine, Jichi Medical School, Tochigi-ken 3290498, Japan*

[3]*Department of Biochemistry, Yokohama City University School of Medicine, Yokohama 236-0004, Japan*

[4]*Center for Biologics Evaluation and Research, US Food and Drug Administration, Bethesda, MD 20892, USA*

*Correspondence to:
Dr Kenji Okuda, Department of Bacteriology, Yokohama City University School of Medicine, 3–9 Fukuura, Kanazawa-ku, Yokohama 236-004 Japan. E-mail: kokuda@med.yokohama-cu.ac.jp

Received: 22 August 2002
Revised: 15 October 2002
Accepted: 24 October 2002

Abstract

Background DNA vaccines have been used to induce both humoral and cellular immune responses against infectious microorganisms. This study explores whether DNA vaccine immunogenicity can be improved by introducing inverted terminal repeats (ITRs) from adeno-associated virus (AAV) into the regulatory region of the DNA plasmid.

Methods CMV promoter-driven HIV Env expressing plasmid (pCMV-HIV) and the pCMV-HIV plasmid introduced ITRs (pITR/CMV-HIV) were transfected in HEK293 cells with LipofectAmine. The HIV Env expression was quantified with Western blot. Fifty μg of pCMV-HIV or pITR/CMV-HIV plasmid with RIBI adjuvant were immunized to BALB/c mice on days 0, 14 and 28 by intramuscular route, and HIV-specific serum IgG titer was detected 2, 6, 10, 14 and 18 weeks after the first immunization. HIV-specific tetramer assay and HIV-specific IFN-γ ELIspot assay were performed 1 week after the last immunization. The immune mice were intravenously challenged with a vaccinia virus expressing the HIV *env* gene 1 week after the last immunization.

Results Significantly higher level of HIV Env expression was achieved by pITR/CMV-HIV plasmid. BALB/c mice immunized with pITR/CMV-HIV plasmid generated significantly higher HIV-specific antibody, higher cellular immune responses and lower viral loading than animals immunized with pCMV-HIV plasmid.

Conclusions AAV ITRs enhance CMV-dependent up-regulation of transgene expression and immunogenicity of DNA vaccine.

Keywords AAV-ITR; DNA vaccine; immune response

Introduction

There is considerable interest in developing plasmid DNA vaccines to prevent or treat infectious diseases, including AIDS. However, results from clinical trials suggest that the immunogenicity of these vaccines in humans may be limited. To date, DNA vaccines alone have failed to prevent the replication of highly virulent HIV strains in non-human primates.

To increase the activity of this class of vaccine, we and others have been exploring the benefit of co-immunizing with various types of vaccine adjuvant [1–4]. Ongoing efforts to increase the immunogenicity of DNA

vaccines include the co-delivery of vectors encoding immunomodulatory cytokines [1,5,6], chemokines [7], co-stimulatory molecules [8], CpG motif [4], chemical agents [2,9], and administering the DNA vaccine in lipid vesicles [10].

Can stronger DNA vaccines be constructed? This study investigates whether introducing inverted terminal repeats (ITRs) from adeno-associated virus (AAV) can improve the immunogenicity of DNA vaccines in a mouse model. AAV is a small, single-stranded DNA virus lacking an envelope. The 4.7-kb genome of AAV contains two 145-bp ITRs. Infected cells convert the single-stranded AAV DNA into a double-stranded transcriptional template which can then integrate into the genome of mammalian cells [11,12]. The AAV ITRs are *cis*-acting elements that promote AAV replication, integration, and excision, but which also enhance the activity of the AAV promoter [13].

To explore whether these ITRs can improve the function of the CMV promoter used to drive expression of the gene(s) encoded by DNA vaccines, plasmids were constructed that expressed either the HIV *env* or *lacZ* gene under the control of the CMV promoter with or without AAV ITRs. Results indicate that both *in vitro* and *in vivo*, addition of the ITRs enhances gene expression and the magnitude of the resultant immune responses.

Materials and methods

Plasmid DNA

The DNA plasmids used in this study are shown in Figure 1. The pCMV-LacZ plasmid was constructed as follows. A 2.7-kb *Kas* I-*Ear* I fragment from pUC19 was blunted and ligated to a multiple cloning sequence containing the restriction enzyme sites 5′-*Not* I-*Mlu* I-*Sna*B I-*Age* I-*Bst*B I-*Bss*H II-*Nco* I-*Hpa* I-*Bsp*E I-*Pml* I-*Rsr* II-*Not* I-3′. The following fragments were successively cloned into the following sites: a *Spe* I-*Sac* II fragment containing the cytomegalovirus (CMV) immediate-early promoter was cloned into the *Sna*B I site, a *Bst*B I-*Bst*B I fragment from the first intron of the human growth hormone was inserted into the *Bst*B I site, multi-cloning fragment (*Cla* I-*Eco*R I-*Sma* I-*Bam*H I-*Xba* I-*Acc* I-*Sal* I-*Bsp*M I-*Pst* I-*Eco*R V-*Xho* I-*Hind* III) was ligated into the *Bss*H II site, and the *Hpa* I-*Bam*H I fragment of the simian virus 40 (SV40) polyadenylation signal sequence was cloned into the *Hpa* I site (pCMV plasmid). The lacZ reporter gene was ligated into the *Eco*R I site of pCMV plasmid to generate pCMV-LacZ plasmid. The pITR/CMV-LacZ plasmid was constructed by inserting the *Not* I-*Not* I expression cassette from pCMV-LacZ plasmid between the AAV 145-bp ITRs of a pUC-based plasmid. The pITR-LacZ plasmid was constructed from a *Spe* I-*Cla* I fragment-deleted pITR/CMV-LacZ plasmid. To construct pCMV-HIV plasmid which expresses both HIV *env* and HIV *rev* genes, an internal ribosome entry site (IRES) fragment was ligated into the *Acc* I-*Bsp*M I site of the pCMV plasmid. Then a 2.5k bp full length HIV *env* gene and a 351 bp full length HIV *rev* gene amplified from pcREV were ligated into the *Eco*R I and *Pst* I-*Xho* I sites of the plasmid to generate the pCMV-HIV plasmid, respectively. The pITR/CMV-HIV plasmid was constructed by inserting the *Not* I-*Not* I expression cassette from the pCMV-HIV plasmid between the AAV 145-bp ITRs. The pITR-HIV plasmid was constructed from a *Spe* I-*Cla* I fragment-deleted pITR/CMV-HIV plasmid.

In vitro expression of the β-galactosidase and HIV *env* genes

Hela, Cos I and/or HEK 293 cells were transfected with 0.5, 2 or 5 μg of plasmid DNA (pCMV-LacZ, pITR/CMV-LacZ or pITR-LacZ) plus LipofectAmine Plus (Invitrogen) according to the manufacturer's instructions. Two days after transfection, gene expression was monitored in triplicate for each sample using a β-gal assay kit

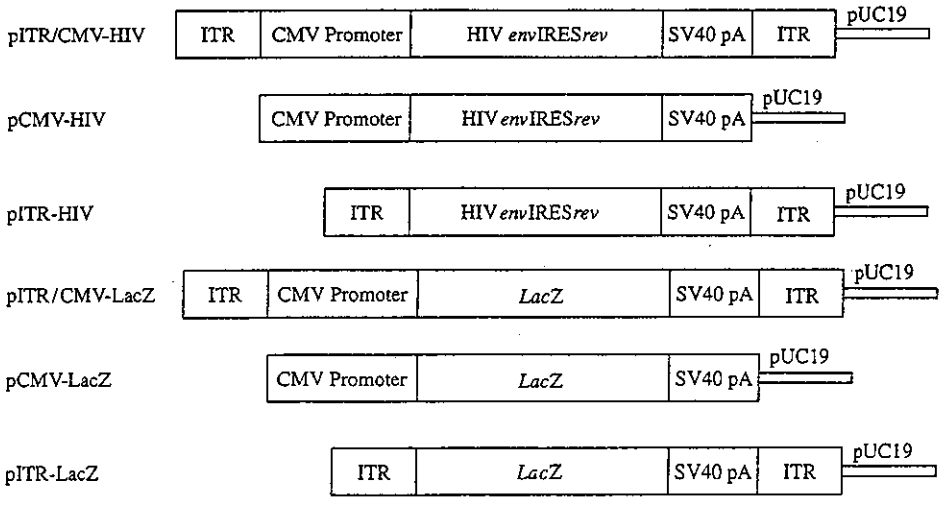

Figure 1. Organization of plasmids used in this study. ITR: inverted terminal repeat; CMV promoter: enhancer and CMV promoter; HIV *env*IRES*rev*: HIV *env*-IRES-HIV*rev*; SV40 pA: SV 40 polyadenylation signal sequence

(Invitrogen) as recommended by the manufacturer. The β-galactosidase activity of cell lysates was calculated using a standard curve generated from a commercial enzyme preparation (*E. coli* β-galactosidase, Sigma).

To explore the transfection efficiency and integration or episomal persistence of ITR-introducing plasmid, at indicated time points post-transfection, part of the transfected cells was used for passage and remaining cells were used for detection of β-galactosidase activity and stained with X-gal. The β-galactosidase activity of cell lysates was calculated from the standard curve derived from the commercial enzyme preparation as above.

To quantify the expression of HIV Env protein, HEK 293 cells were transfected as described above with 0.5, 2 or 5 μg of plasmid (pCMV-HIV, pITR/CMV-HIV, pITR-HIV or pCMV-empty). Two days after transfection, the cells were washed in phosphate-buffered saline (PBS) and lysed in 50 mM Tris-HCl (pH 7.8) with 1% Nonidet P-40. The protein concentration of lysates was measured with a Bio-Rad protein assay kit. Cell lysates (10 μg) were loaded onto a 4–12% gradient polyacrylamide gel followed by transfer to Hybond ECL nitrocellulose membrane (Amersham Pharmacia Biotech, Bucks, UK). The protein was detected using the HIV-1 IIIB gp120 specific mouse hybridoma 902 (AIDS Research and Reference Reagent Program, MD, USA). An anti-β-actin mAb was used as an internal control antibody (AC-15; Sigma). An affinity-purified horseradish peroxidase (HRP)-labeled anti-mouse Ig Ab was used as the secondary Ab. The density of the protein bands was quantified using Image Gange software (version 3.0; Fujifilm, Tokyo, Japan). The ratio of HIV Env protein was calculated as (β-actin density of pITR/CMV-HIV × HIV Env density of pCMV-HIV)/β-actin density of pCMV-HIV). The HIV Env density included both density of gp120 and gp160.

Animals and animal immunization

Eight-week-old BALB/c female mice were purchased from Japan SLC. Inc. (Shizuoka, Japan). The mice were housed in the Animal Center of Yokohama City University where they were kept on a 12-h day/night cycle. Mice were intramuscularly immunized with 50 μg of plasmid plus 5 μl RIBI adjuvant in PBS on days 0, 14 and 28.

Sample collection and ELISA

Serum Abs were detected by ELISA, as previously described [14]. Briefly, 96-well microtiter plates were coated with 10 μg/ml of HIV V3 region peptide (NNTRKRIQRGPGRAFVTIGKIGN-multi-antigen peptide, HIV V3-MAP peptide) at 4 °C overnight. The wells were blocked with PBS containing 1% bovine serum albumin (BSA) and incubated for 2 h at room temperature. Serial two-fold dilutions of antisera were added for an additional hour at 37 °C. The bound Ab was detected using HRP-labeled anti-mouse IgG antibody (Sigma). The mean antibody titer was expressed as the reciprocal of the serial serum dilution that reached the cut-off value plus 2 SD.

IFN-γ ELIspot assay and computer-assisted video image analysis (CVIA)

IFN-γ ELIspot assays were performed 1 week after the final immunization, as previously described [15]. Briefly, MultiScreen-IP plates (Millipore, Bedford, MA, USA) were coated with 50 μl of 10 μg/ml of rat anti-mouse IFN-γ antibody in PBS (XMG1.2; Pharmingen, CA, USA) overnight at 4 °C. The plate was then blocked with RPMI1640 medium with 10% FCS for 2 h at room temperature. Lymphocytes ($1–10 \times 10^5$) from the spleen were added to each well, in triplicate. To monitor HIV-specific IFN-γ production, spleen cells were stimulated with 10 μg/ml of HIV V3 peptide (NNTRKRIQRGPGRAFVTIGKIGN) for 20 h at 37 °C. Control wells contained non-stimulated cells. After incubation, cells were removed and the wells incubated with 0.5 μg/ml of biotinylated anti-mouse IFN-γ antibody (Pharmingen) for 2 h at 37 °C, followed by adding 100 μl/well of 0.2% alkaline phosphatase streptavidin (Vector, CA, USA) in PBS containing 0.05% Tween-20 and 0.5% BSA for 1.5 h. Finally, the plate was treated with 50 μl/well of BCIP/NBT membrane phosphatase (Kirkegaare and Perry Laboratories, MD, USA) at room temperature for 20 min and the reaction was stopped under running distilled water. The numbers of spots were automatically determined by CVIA [16].

Tetramer assay

The tetramer assay was performed 1 week after the final boost. The H-2D/p18 tetramer (RGPGRAFVTI) labeled with PE was provided by the NIH AIDS Research and Reference Reagent Program. The H-2k(d)/NP tetramer (TYQRTRALV, influenza NP gene, PR8 strain) was used as a negative control tetramer reagent. The tetramer assay was performed as previously described [17]. Briefly, mouse splenocytes were incubated for 30 min at 4 °C with 4% normal mouse serum in PBS. Cells were stained with fluorescein isothiocyanate (FITC)-labeled anti-mouse CD8a antibody (Ly-2, Pharmingen) at 0.5 μg/10^6 cells for 30 min at 4 °C. After being washed twice with staining buffer (3% FCS, 0.1% NaN_3 in PBS), the cells were incubated with the tetramer reagent for 15 min at 37 °C followed by flow cytometric analysis.

Recombinant vaccinia virus used for challenge studies

The virus challenge experiment was performed 1 week after the last immunization as described previously [18]. Recombinant vaccinia virus vPE16 expressing the HIV-1 *env* gene (Cat. No. 362; NIH AIDS Reagent Program

and Reference Reagent Program) was used for the study. Briefly, 1 week after immunization, mice were challenged intravenously with 5×10^7 plaque-forming units (pfu) of vPE16 vaccinia virus. Six days after the challenge with the recombinant vaccinia virus, the mice were sacrificed, and ovaries were removed, sonicated, and assayed for vPE16 titer by plating serial 10-fold dilution on a plate of CV1 cells, staining with crystal violet and counting plaques at each dilution.

Data analysis

All values are expressed as means ± standard error (S.E.). Statistical analysis of the experimental data and controls was conducted with one-way factorial analysis of variance. Significance was defined at $p < 0.05$ in statistical analyses.

Results

Addition of ITRs improves gene expression by DNA plasmids

To examine the effect of AAV ITRs on transgene expression, we prepared several constructs. As shown in Figure 1, the pITR/CMV-HIV and pCMV-HIV express full length of the HIV *env* and *rev* genes, which was controlled by CMV promoter with or without ITRs; the pITR-HIV contains AAV ITRs but lacks the CMV promoter. The HIV gene was replaced with a reporter gene, *lacZ*, to generate pITR/CMV-LacZ, pCMV-LacZ and pITR-LacZ for qualifying the protein expression. Hela, Cos I and HEK 293 cells were transfected with 2 μg each of pITR/CMV-LacZ, pCMV-LacZ or pITR-LacZ plasmid using LipofectAmine. Two days later, β-galactidase protein levels were measured. As seen in Figure 2, β-galactosidase activity was greatest in all three kinds of cell types transfected with pITR/CMV-LacZ, suggesting that the addition of the ITR to the pCMV-LacZ construct enhanced gene expression. Cells transfected with pITR-LacZ expressed no detectable enzyme activity. To explore whether the β-galactosidase activity was dependent on DNA plasmid dose, we transfected with 0.5 or 5 μg each of *lacZ*-containing DNA plasmid. A similar pattern of β-galactosidase activity was observed as with the one transfected with 2 μg of DNA plasmid (data not shown). This set of observations suggests that the ITR acts to enhance CMV promoter function, which is independent of the transfected DNA plasmid dose.

The HIV Env protein expression of plasmids was also quantified by Western blot. HEK 293 cells were transfected with 2 μg each of pITR/CMV-HIV, pCMV-HIV, pITR-HIV or mock pCMV plasmid. Results indicate that pITR/CMV-HIV-tranfected cells produced 1.8-fold more Env than pCMV-HIV-transfected cells (Figure 3). No HIV Env protein was detected in cells transfected with the

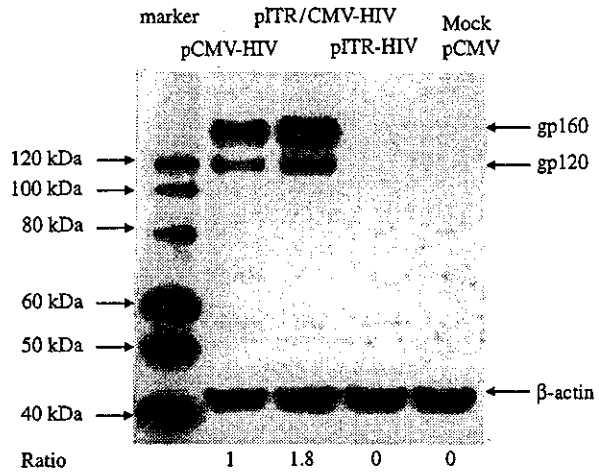

Figure 3. Quantification of HIV Env protein by Western blot. DNA plasmid (2 μg each) was transfected into HEK 293 cells. The amount of HIV Env protein in the lysates of HEK 293 cells transfected 2 days earlier was analyzed by Western blot. When 0.5 or 5 μg of DNA plasmid was used, HIV Env expression ratio of pITR/CMV-HIV to pCMV-HIV was similar to using 2 μg of DNA plasmid. Another two separate experiments showed similar results

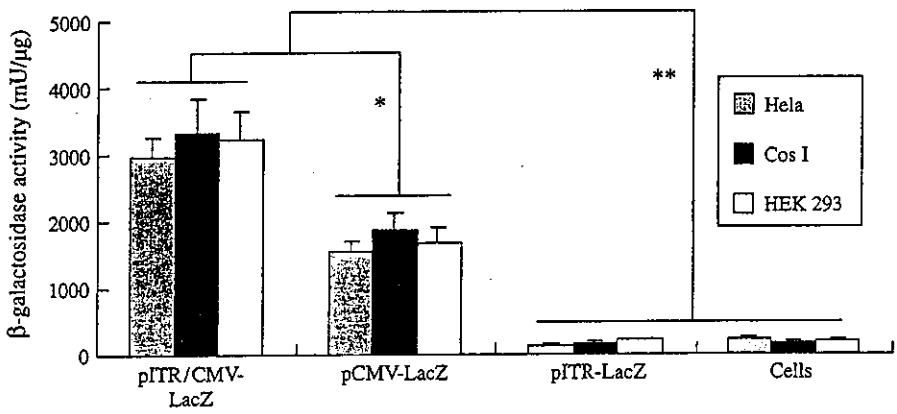

Figure 2. β-Galactosidase activity in transfected cell lines. The β-galactosidase activity was measured 2 days after LipofectAmine-mediated transfection of DNA plasmid, in triplicate for each sample. Data represent the average of 2–3 separate experiments. *, **Mean values significantly different from the two groups

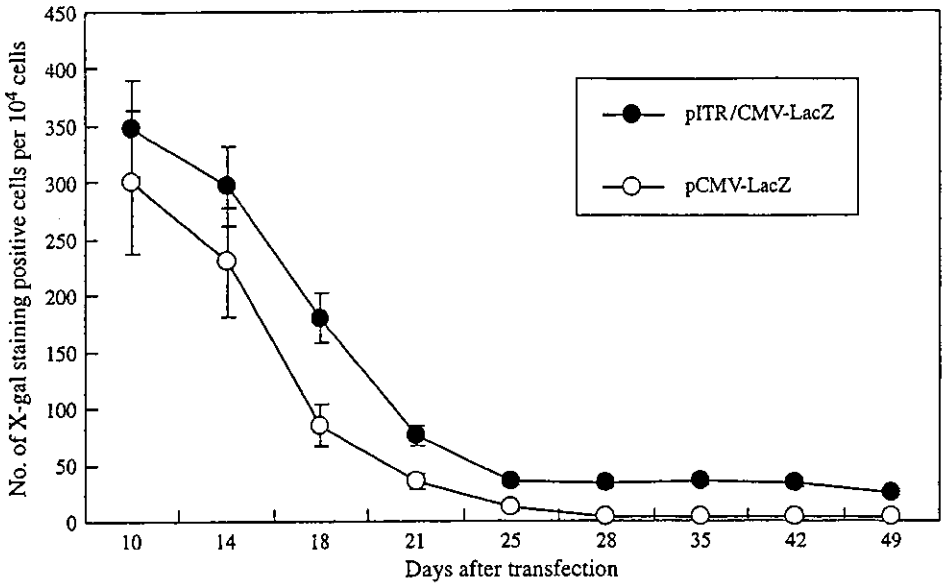

Figure 4. Long-term transfection study. HEK 293 cells were transfected with 2 μg of pITR/CMV-LacZ and pCMV-LacZ. At indicated time points, the cells were stained with X-gal and LacZ-positive cells were counted. Data are the average of two separate experiments

pITR-HIV or the mock plasmid. Furthermore, using anti-HIV Env mAb and anti-HIV Rev mAb alone did not bind to HIV Rev and HIV Env proteins, respectively. When 0.5 or 5 μg of each HIV Env-expressing plasmid was transfected into HEK 293 cells, similar HIV Env expression ratio of pITR/CMV-HIV to pCMV-HIV to using 2 μg DNA was observed (data not shown). These findings confirm the results shown in Figure 2, indicating that the ITR enhances CMV promoter function, which is independent of the transfected DNA plasmid dose.

The AAV ITRs are *cis*-acting elements that promote AAV integration to the host genome. To investigate whether the higher β-galactosidase activity of the pITR/CMV-LacZ was the result of chromosomal integration and/or episomal persistence, we transfected the pITR/CMV-LacZ or pCMV-LacZ plasmid to HEK 293 cells; cells were stained with X-gal at each passage and positive cells were counted. As shown in Figure 4, positive cells were greatly decreased from 10 days after transfection (usually we obtained 70% positive cells 2 days after transfection). Slightly higher numbers of positive cells were obtained in the pITR/CMV-LacZ-transfected cells than the pCMV-LacZ-transfected cells. By 49 days after transfection, there were 25 and 3 positive cells out of 10^4 cells in pITR/CMV-LacZ- and pCMV-LacZ-transfected cells, respectively. These data indicate that AAV ITRs may increase the chromosomal integration or episomal persistence.

Induction of HIV-specific immune responses *in vivo*

BALB/c mice were immunized and boosted twice with each HIV plasmid DNA construct. Analysis of the resultant serum Ab response showed that the antigen-specific IgG response peaked 10 weeks after the first immunization (Figure 5). The pITR/CMV-HIV plasmid induced significantly higher HIV-1-specific antibody than did any of the other plasmids examined.

ELIspot and tetramer assays were used to examine the effect of vaccination on Env-specific T cell activation. Mice immunized with pITR/CMV-HIV generated significantly more IFN-γ ELIspots (which reflect antigen-specific CTL activity) than animals immunized with pCMV-HIV (610 vs. 280 spots/10^6 cells, $p < 0.05$, Figure 6). Both of these treatments generated significantly more HIV-specific IFN-γ-secreting splenocytes than were present in the non-immune group (23 spots/10^6 cells) or pCMV-lacZ-immunized group (25 spots/10^6 cells). By use of a tetramer-binding assay (Figure 7), pITR/CMV-HIV plasmid induced two-fold more HIV Env-specific T cells than pITR/CMV-HIV (0.41% vs. 0.22%, $p < 0.05$).

Challenge experiments with vaccinia virus

To investigate whether the DNA vaccines can induce protective immunity against viral infection, the immune mice were intravenously challenged with recombinant vaccinia virus expressing the HIV *env* gene. DNA vaccines significantly reduced the viral loading (Figure 8); furthermore, the mice immunized with pITR/CMV-HIV plasmid showed more than five-fold lower viral loading than the mice with pCMV-HIV plasmid.

Discussion

Current results indicate that introduction of an AAV ITR into the regulatory region of plasmid DNA vaccines enhances CMV promoter activity, increases expression

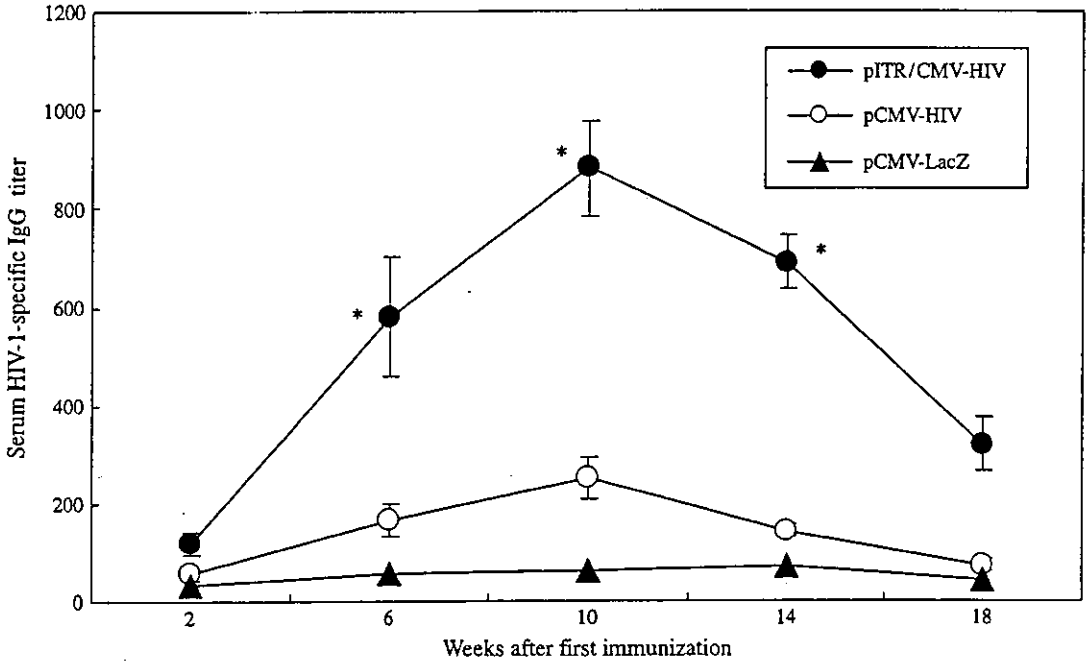

Figure 5. Anti-HIV serum IgG titers. Mice were immunized at 0, 2, and 4 weeks, and HIV-specific serum IgG titers monitored through week 18. Data represent the average of 5 mice/group. *Mean values significantly different from animals treated with pITR/CMV-HIV and pCMV-HIV plasmids

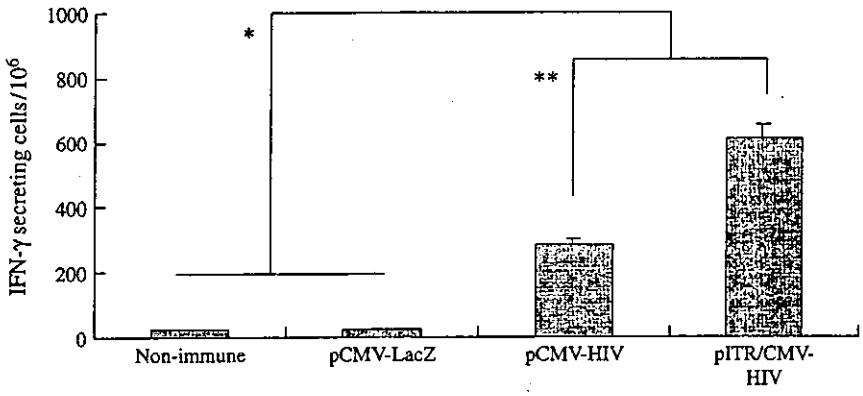

Figure 6. IFN-γ response of immunized mice. Mice were immunized as described in Figure 5. One week after the last immunization, spleen cells were isolated and stimulated *in vitro* with V3 peptide. The number of antigen-specific IFN-γ-secreting lymphocytes was determined by ELIspot assay. Data represent the average of 4 mice/group. *Mean values significantly different from animals treated with HIV Env-expressing plasmid and controls. **Mean values significantly different from animals treated with pITR/CMV-HIV and pCMV-HIV plasmids

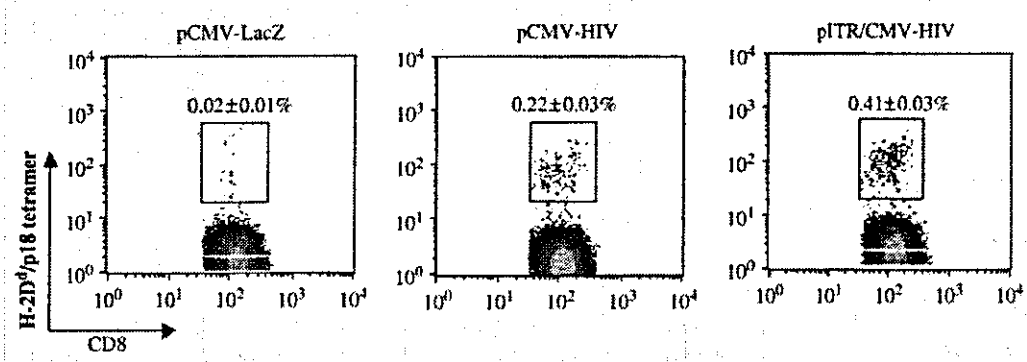

Figure 7. Frequency of HIV-specific CD8$^+$ spleen cells. Spleen cells from mice treated as described in Figure 6 were stained for CD8 expression, and for expression of TCR that recognized the MHC class I-restricted p18 tetramer from HIVgp160. Data represent the average of six mice

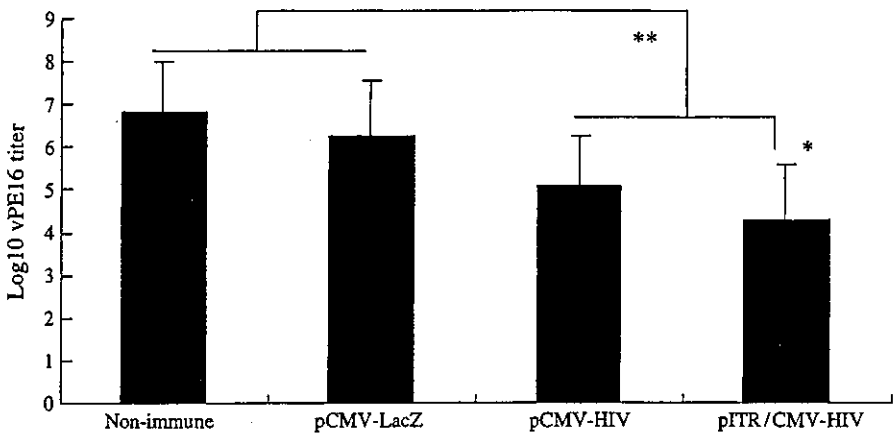

Figure 8. Resistance of immunized mice to infection by vaccinia virus (vPE16) expressing the HIV *env* gene. One week after the last immunization, immune mice were challenged intravenously with 5×10^7 pfu of vPE16 virus. Vaccinia virus titers were measured 6 days after virus challenge. Data represent the average of 10 mice/group

of the encoded antigen, and thereby boosts vaccine immunogenicity. Introducing these ITRs into plasmids encoding the *Lac*Z or HIV *env* gene under the control of a CMV promoter significantly enhanced protein production (Figures 2 and 3). The effect of the ITR was mediated by the CMV promoter, since no effect was observed in plasmids containing ITR but not CMV. Mice immunized with ITR-enhanced plasmids generated significantly higher antigen-specific Ab and cell-mediated immune responses (Figures 5, 6 and 7).

Current results confirm and extend earlier observations establishing that plasmids encoding ITRs can efficiently transfect host cells, and induce protein expression [19,20]. Furthermore, ITR-introduced DNA vaccine induces higher antigen-specific immune responses *in vivo*. Our findings are also in general agreement with data from Flotte *et al.* indicating that the ITR sequence can enhance the functional activity of the AAV p5 promoter [21]. Indeed, in our hands, AAV-ITR alone did not significantly promote gene expression (Figures 2 and 3). Additional studies performed in our laboratory confirm that plasmid introducing the AAV ITR but lacking the CMV promoter is virulently inactive (data not shown).

The mechanism of AAV integration is not yet fully understood. Recombinant AAV randomly integrates its transgene into mammalian cells [22–25], but most of them apparently as an episomal form for long-term expression [26]. To investigate whether the higher expression in the ITR-introducing plasmid was caused by chromosomal integration or episomal persistence, we transfected the pCMV-LacZ and pITR/CMV-LacZ plasmid into HEK 293 cells and counted LacZ-positive cells for 49 days. We found that the amount of positive cells was rapidly reduced in each plasmid-transfected cells by 21 days and positive cells in pITR/CMV-LacZ-transfected cells were 15–20% higher than the pCMV-LacZ-transfected cells. However, by 49 days post-transfection, there were 25 and 4 positive cells per 10^4 cells using pITR/CMV-LacZ and pCMV-LacZ, respectively (Figure 4). These results suggest that ITRs of plasmid without AAV helper components may play a role in chromosomal integration or episomal persistence. Single-stranded AAV genome has to be synthesized to double-stranded DNA then integrate to the host genome. Therefore, double-stranded DNA plasmid with ITRs may be more efficient for chromosomal integration than the single-stranded AAV genome *in vivo* [27]. In this study, we are not sure whether the increased chromosomal integration or episomal persistence greatly affected immunogenicity of the HIV vaccines with or without ITRs, since the number of positive cells was not high (Figure 4).

To increase the DNA vaccine-induced HIV-specific immune responses, RIBI adjuvant, a detoxified form of lipid A derived from the lipopolysaccharide of *Salmonella Minnesota* R595, was used as a vaccine adjuvant [28]. Early studies [29,30] showed that the adjuvant activity of RIBI reflects its ability to activate macrophages and stimulate IFN-γ and interleukin 2 (IL-2) [31] production, known to be essential for the induction of Th1-derived cell-mediated immunity. Moreover, inclusion of RIBI improved the transfection efficiency of pITR/CMV-LacZ and pCMV-LacZ into HEK 293 cells (data not shown).

Taken together, current results indicate that DNA vaccines containing both AAV ITRs and the CMV promoter induce higher antigen-specific antibody and IFN-γ responses than vaccines with a CMV promoter alone, and that AAV ITRs act by enhancing the activity of the CMV promoter rather than a promoter itself.

Acknowledgements

We are grateful to Ms. M. Kawano for her technique assistance and Ms. T. Takeishi and A. de la Fuente for their secretarial assistance. We also extend our appreciation to Avigen, Inc. (Alameda, CA, USA) for supplying the AAV plasmids used in this study. This work was partially supported by a Grant-in-Aid from the Ministry of Education, Science, Sports, Culture of Japan, the Ministry of Health and Welfare of Japan and the Japan Health Sciences Foundation (SA24713).

References

1. Xin K-Q, Hamajima K, Sasaki S, *et al.* IL-15 expression plasmid enhances cell-mediated immunity induced by an HIV-1 DNA vaccine. *Vaccine* 1999; 17: 858–866.
2. Sasaki S, Fukushima J, Hamajima K, *et al.* Adjuvant effect of ubenimex on a DNA vaccine for HIV-1. *Clin Exp Immunol* 1998; 111: 30–35.
3. Okuda K, Xin K-Q, Tsuji T, *et al.* DNA vaccination followed by macromolecular multicomponent peptide vaccination against HIV-1 induces strong antigen-specific immunities. *Vaccine* 1997; 15: 1049–1056.
4. Kojima Y, Xin K-Q, Ooki T, *et al.* Adjuvant effect of multi-CpG motifs on an HIV-1 DNA vaccine. *Vaccine* 2002; 20: 2857–2865.
5. Tsuji T, Hamajima K, Fukushima J, *et al.* Enhancement of cell-mediated immunity against HIV-1 induced by coinoculation of plasmid-encoded HIV-1 antigen with plasmid expressing interleukin-12. *J Immunol* 1997; 158: 4008–4013.
6. Xin K-Q, Hamajima K, Sasaki S, *et al.* Intranasal administration of HIV-1 DNA vaccine with IL-2 expression plasmid enhances cell-mediated immunity against HIV-1. *Immunology* 1998; 94: 438–444.
7. Xin K-Q, Lu Y, Hamajima K, Yang J, Inamura K, Okuda K. Immunization of RANTES expression plasmid with a DNA vaccine enhances HIV-1-specific immunity. *Clin Immunol* 1999; 92: 90–96.
8. Tsuji T, Hamajima K, Ishi N, *et al.* Immunodulatory effects of plasmid expressing B7-2 on human immunodeficiency virus-1 specific cell-mediated immunity induced by plasmid-encoded the viral antigen. *Eur J Immunol* 1997; 27: 782–787.
9. Sasaki S, Hamajima K, Fukushima J, *et al.* A comparison of intranasal and intramuscular DNA vaccination against human immunodeficiency virus type 1 with monophosphoryl lipid A adjuvant. *Infect Immunol* 1998; 66: 823–826.
10. Ishii N, Fukushima J, Kaneko T, *et al.* Cationic liposomes are a strong adjuvant for a human immunodeficiency virus type-1 (HIV-1) vaccine candidate constructed with HIV-1 env and rev genes. *AIDS Res Hum Retrov* 1997; 13: 1421–1428.
11. Kearns WG, Afione SA, Fulmer SB, *et al.* Recombinant adeno-associated virus (AAV-CFTR) vectors do not integrate in a site-specific fashion in an immortalized epithelial cell line. *Gene Ther* 1996; 3: 748–755.
12. Afione SA, Conrad CK, Kearns WG, *et al.* In vivo model of adeno-associated virus vector persistence and rescue. *J Virol* 1996; 70: 3235–3241.
13. Ozawa K. *Parvovirus, Virology*, Hatanaka S (ed). Asakura Press: Tokyo, 1997; 222–229.
14. Xin KQ, Urabe M, Yang J, *et al.* A novel recombinant adeno-associated virus vaccine induces a long-term humoral immune response to HIV. *Hum Gene Ther* 2001; 12: 1047–1061.
15. Xin K-Q, Sasaki S, Kojima Y, *et al.* Detection of progeny immune responses after intravenous administration of DNA vaccine to pregnant mice. *Biol Proc Online* 2002; 3: 91–101. Available: www.biologicalprocedures.com.
16. Herr W, Linn B, Leister N, Wandel E, Buschenfelde KHMZ, Wolfel T. The use of computer-assisted video image analysis for the quantification of $CD8^+$ T lymphocytes producing tumor necrosis factor α spots in response to peptide antigens. *J Immunol Methods* 1997; 203: 141–152.
17. Xin K-Q, Ooki T, Mizukami H, *et al.* Oral administration of recombinant adeno-associated virus elicits HIV-specific immune responses. *Hum Gene Ther* 2002; 13: 1571–1581.
18. Belyakov IM, Derby MA, Ahlers JD, *et al.* Mucosal immunization with HIV-1 peptide vaccine induces mucosal and systemic cytotoxic T lymphocytes and protective immunity in mice against intrarectal recombinant HIV-vaccinia challenge. *Proc Natl Acad Sci U S A* 1998; 95: 1709–1714.
19. Philip R, Brunette E, Kilinski L, *et al.* Efficient and sustained gene expression in primary T lymphocytes and primary and cultured tumor cells mediated by adeno-associated virus plasmid DNA complexed to cationic liposomes. *Mol Cell Biol* 1994; 14: 2411–2418.
20. Vieweg J, Boczkowski D, Roberson KM, *et al.* Efficient gene transfer with adeno-associated virus-based plasmids complexed to cationic liposomes for gene therapy of human prostate cancer. *Cancer Res* 1995; 55: 2366–2372.
21. Flotte TR, Afione SA, Conrad C, *et al.* Stable in vivo expression of the cystic fibrosis transmembrane conductance regulator with an adeno-associated virus vector. *Proc Natl Acad Sci U S A* 1993; 90: 10 613–10 617.
22. Pieroni L, Fipaldini C, Monciotti A, *et al.* Targeted integration of adeno-associated virus-derived plasmids in transfected human cells. *Virology* 1998; 249: 249–259.
23. Linden RM, Winocour E, Berns KI. The recombination signals for adeno-associated virus site-specific integration. *Proc Natl Acad Sci U S A* 1996; 93: 7966–7972.
24. Dutheil N, Shi F, Dupressoir T, Linden M. Adeno-associated virus site-specifically integrates into a muscle-specific DNA region. *Proc Natl Acad Sci U S A* 2000; 97: 4862–4866.
25. Rizzuto G, Gorgoni B, Cappelletti M, *et al.* Development of animal models for adeno-associated virus site-specific integration. *J Virol* 1999; 73: 2517–2526.
26. Nakai H, Yant SR, Storm TA, *et al.* Extrachromosomal recombinant adeno-associated virus vector genomes are primarily responsible for stable liver transduction *in vivo*. *J Virol* 2001; 75: 6969–6976.
27. Nakai H, Montini E, Fuess S, *et al.* Helper-independent chromosomal integration of naked double-stranded linear DNA vectors in mice. *Proc Japan Soc Gene Therapy*, Tokyo, July 18–20, 2002.
28. Ulrich JT, Myers KR. Monophosphoryl lipid A as an adjuvant. Past experiences and new directions. In *Vaccine Design*, Powell MF, Newman MJ (eds). Plenum Press: New York, 1995; 495–523.
29. Rickman LS, Gordon DM, Wistar RJ, *et al.* Use of adjuvant containing mycobacterial cell-wall skeleton, monophosphoryl lipid A, and squalane in malaria circumsporozoite protein vaccine. *Lancet* 1991; 337: 998–1001.
30. Gustafson GL, Rhodes MJ. Bacterial cell wall products as adjuvants: early interferon gamma as a marker for adjuvants that enhance protective immunity. *Res Immunol* 1992; 143: 483–488.
31. Mosmann TR, Cherwinski H, Bond MW, Giedlin MA, Coffman RL. Two types of murine helper T cell clone. 1. Definition according to profiles of lymphokine activities and secreted proteins. *J Immunol* 1986; 136: 2348–2357.

ELSEVIER

Neuroscience Letters 340 (2003) 153–157

Neuroscience Letters

www.elsevier.com/locate/neulet

Distinct patterns of gene transfer to gerbil hippocampus with recombinant adeno-associated virus type 2 and 5

Tatsuya Nomoto[a,b], Takashi Okada[a], Kuniko Shimazaki[c], Hiroaki Mizukami[a], Takashi Matsushita[a], Yutaka Hanazono[a], Akihiro Kume[a], Ken-ichiro Katsura[b], Yasuo Katayama[b], Keiya Ozawa[a,*]

[a]*Division of Genetic Therapeutics, Center for Molecular Medicine, Jichi Medical School 3311-1 Yakushiji, Minami-kawachi, Kawachi, Tochigi 329-0498, Japan*

[b]*Second Department of Internal Medicine, Nippon Medical School, 1-1-5 Sendagi, Bunkyo-ku, Tokyo 113-8603, Japan*

[c]*Department of Physiology, Jichi Medical School 3311-1 Yakushiji, Minami-kawachi, Kawachi, Tochigi 329-0498, Japan*

Received 26 December 2002; received in revised form 9 January 2003; accepted 10 January 2003

Abstract

Genetic modification of the gerbil hippocampal neuronal cells in vivo helps us understand the mechanisms of neuronal function under various circumstances such as ischemic insult. In this study, we examined the distinct distribution of the recombinant adeno-associated virus type 2 (rAAV2) and rAAV5 vectors for gene delivery to primary cultured cells and the gerbil hippocampus. Mixed cortical cultures containing both neurons and astrocytes from E17 rat embryos were infected with rAAVs containing the Cytomegalovirus virus (CMV) promoter. rAAV2 was preferably transduced to neurons, whereas rAAV5 was inclined to be transduced to astrocytes in vitro. rAAV2 and rAAV5 vectors, each with the CMV or Rous sarcoma virus (RSV) promoter, were injected into the gerbil hippocampus using a stereotaxic apparatus. Five days after injection, transgene expression was analyzed with X-gal staining. In the gerbil hippocampus, rAAV5 with the CMV promoter achieved a higher overall transgene expression than rAAV2 with the CMV promoter. The transgene expression of rAAV2 with the RSV promoter was found in the pyramidal and granular cells, while the transgene expression of rAAV5 with the RSV promoter was preferentially found in the granular cells. These findings would be valuable in optimizing rAAV-mediated gene transfer to the gerbil hippocampus.

Keywords: Adeno-associated virus; Serotype; Gene transfer; Hippocampus; Gerbil

Considerable interest has been focused on the possible use of viral vectors to deliver genes to the central nervous system (CNS) for the treatment of neuronal injuries. Adeno-associated virus (AAV) is a potentially useful gene transfer vehicle for neurological gene therapies [14,16]. Advantages of the AAV vector include the lack of any associated disease with the wild-type virus, the ability to transduce non-dividing cells including neuronal cells, a minimal immunological response, and the ability to confirm long-term expression of transgenes. The development of novel therapeutic strategies for treating CNS diseases using the AAV vector is having a growing impact on gene therapy research. Development of the AAV vector for use in gene therapy treatment of neuronal diseases has progressed rapidly. Recent findings have shown that recombinant AAV type 5 (rAAV5) can efficiently transduce both neuronal cells and glial cells, while rAAV2 preferentially transduces neuronal cells. Cerebral parenchymal gene transduction by rAAV5 is more diffuse and widespread compared to transduction by rAAV2 [2,9]. Since the homology between AAV2 and AAV5 in both the viral inverted terminal repeats and capsid protein is only about 60% [1], it is speculated that the capsid structure may be responsible for the improved transduction efficiency of AAV5 [4,19].

The Mongolian gerbil is widely used as a model of ischemic neuronal death. Transient occlusion of the carotid arteries in this rodent causes cell death in CA1 pyramidal neurons with a delay of a few days after reperfusion [7,13].

* Corresponding author. Tel.: +81-285-58-7402; fax: +81-285-44-8675.
E-mail address: kozawa@ms.jichi.ac.jp (K. Ozawa).

0304-3940/03/$ - see front matter © 2003 Elsevier Science Ireland Ltd. All rights reserved.
doi:10.1016/S0304-3940(03)00095-8

AAV vectors can be used to identify the specific activity of the gene of interest in vivo to elucidate the pathophysiological reaction to ischemic neuronal insult. Since specific regions of the hippocampus each have distinct functions [6], transgene expression must be regulated in a cell type-specific and region-specific manner to achieve a maximal therapeutic benefit. However, the local distribution pattern of transgene expression with rAAV5 in the hippocampal region has not yet been scrutinized. Here we report on the transduction efficiencies and tropisms in the hippocampus of recombinant virus vectors derived from AAV2 and AAV5 in the gerbil brain.

A schematic representation of the AAV vectors is shown in Fig. 1. Four AAV vectors expressing β-galactosidase were produced as follows: AAV2CMVLZ (rAAV2 with Cytomegalovirus virus (CMV) promoter), AAV5CMVLZ (rAAV5 with CMV promoter), AAV2RSVLZ (rAAV2 with Rous sarcoma virus (RSV) promoter), and AAV5RSVLZ (rAAV5 with RSV promoter). Mixed cortical cultures containing both neurons and astrocytes were prepared from the cerebral cortex of gestation day 17 Wistar rat embryos. After 7 days, the cultured cells were infected with 3.0×10^{10} particles of either AAV2CMVLZ or AAV5CMVLZ per well and incubated for 72 h. Transgene expression was detected by 5-bromo-4-chloro-3-indolyl β-D-galactoside (X-Gal) cytochemical staining. Immunofluorescent staining was performed immediately following X-gal staining. Anti-MAP-2 (Chemicon International, Inc., Temecula, CA) and anti-glial fibrillary acidic protein (GFAP) (Sanbio b.v., AM Uden, Netherlands) were used as primary antibodies at 1:1000 dilution in blocking solution. Alexa-488 and Alexa-564 conjugated secondary antibodies (Molecular Probes, Inc. Eugene, OR) were used at 1:1000 dilution in blocking solution. The proportions of microtubule-associated protein-2 (MAP2)-positive cells (red) and GFAP-positive cells (green) in each experiment were estimated to be 70% and 30%, respectively (Fig. 2A). Although both AAV2CMVLZ and AAV5CMVLZ efficiently transduced to the neurons, AAV2CMVLZ had a higher affinity for MAP2-positive cells than AAV5CMVLZ (Fig. 2B; $P < 0.01$, Mann–Whitney nonparametric test). In contrast, AAV5CMVLZ transduction to GFAP-positive cells was significantly higher than AAV2CMVLZ (Fig. 2B; $P < 0.01$, Mann–Whitney nonparametric test).

We further investigated transgene expression in the gerbil hippocampus in vivo. Taking into consideration that gene transfer to the gerbil hippocampus may be desired for neuronal protection from short-term ischemic insult, transgene expression was analyzed over a short period. Male Mongolian gerbils were anesthetized with 2.5% chloral hydrate (400 mg/kg, i.p.) and then placed in a stereotaxic frame (Type SR-50 NARISHIGE, Tokyo, Japan). A burr-hole was drilled into the pericranium. For the injection of rAAV into the hippocampus, a glass micropipette was placed 1.5 mm below the pia mater via the burr-hole, 2.8 and 3.8 mm to the right, and 1.8 and 3.8 mm posterior to the bregma. rAAV2 and rAAV5 vectors each with either the CMV or RSV promoter (4.25×10^9–6.0×10^{10} particles/5 μl) were injected through a glass micropipette at a rate of 0.25 μl/min using a microinfusion pump. Five days after injection, the gerbils were perfused with 0.9% NaCl under pentobarbital anesthesia followed by 4% paraformaldehyde dissolved in 0.1 mol/l phosphate buffer (PB). The brains were removed and preserved overnight in fixative, then transferred to 0.1 mol/l PB containing 15% sucrose. Coronal sections of the brains were made with a frozen microtome at 50 μm. The sections were stained with the Hist Mark X-gal detection kit (Kirkegaard & Perry Laboratories, Inc., Gaithersburg, MD) as described in the manufacturer's protocol (Fig. 3A–D). The hippocampal expression pattern was quite distinct for each serotype and each promoter. The β-galactosidase expression of AAV2CMVLZ is shown in Fig. 3A. In the stratum oriens, there were many stained cells with large

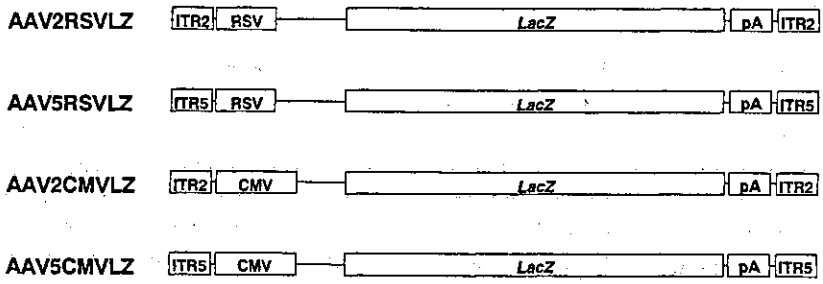

Fig. 1. A schematic representation of the construction of the four different AAV vectors used in this study. rAAV5 expressing the nucleus-targeted Escherichia coli β-galactosidase (β-gal) gene driven by the RSV promoter (AAV5RSVLZ) was generated using the previously described pAAV5RNL proviral plasmid [2]. A proviral plasmid for rAAV2 expressing the nucleus-targeted β-gal gene (AAV2RSVLZ) driven by the RSV promoter was generated from pAAV5RNL. rAAV2 expressing the β-gal gene driven by the CMV promoter (AAV2CMVLZ) was generated using the previously described pAAVLacZ [11]. The proviral plasmid for rAAV5 expressing β-gal gene driven by the CMV promoter (AAV5CMVLZ) was generated from pAAVLacZ. The rAAV viral stocks were propagated according to a previously described three-plasmid transfection adenovirus-free protocol [10]. Briefly, 60% confluent 293 cells were co-transfected with the proviral plasmid, AAV helper plasmid pHLP19 [11] (for rAAV2) or pAAV5RepCap [1] (for rAAV5), and adenoviral helper plasmid pAdeno. The crude viral lysate was purified through two rounds of CsCl two-tier centrifugation. The physical titer of the viral stock was determined by dot blot hybridization with plasmid standards. ITR2, ITR5: inverted terminal repeats of AAV2 or AAV5; RSV, Rous sarcoma virus promoter; CMV, Cytomegalovirus promoter; LacZ, lacZ coding sequence; pA, SV40 polyadenylation signal.

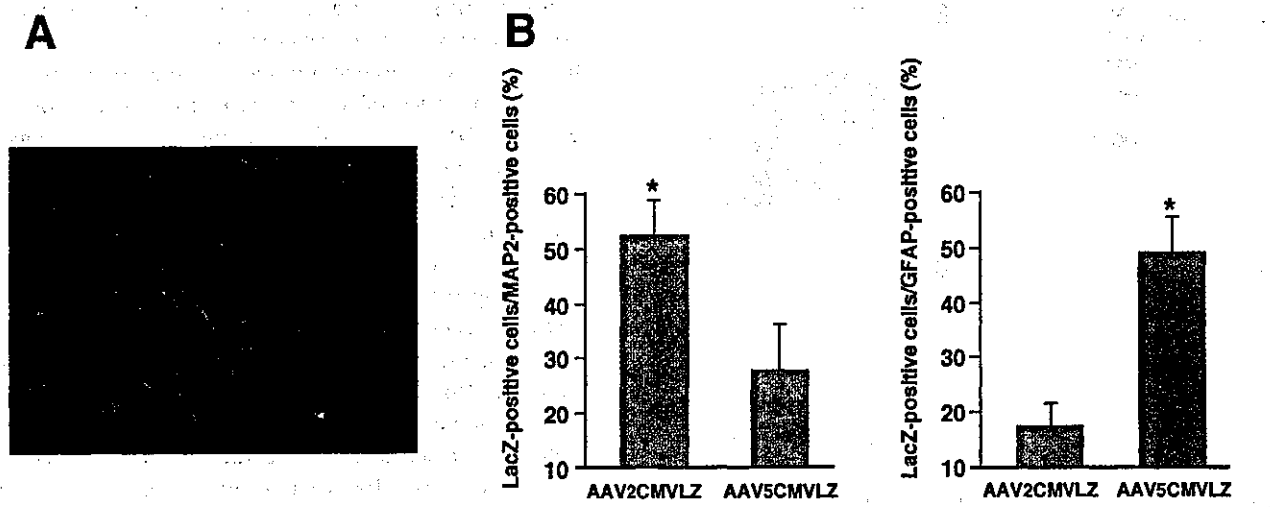

Fig. 2. Transduction efficiency of primary cultured rat cortical cells with rAAVs. Mixed cortical cultures containing both neurons and astrocytes were prepared from the cerebral cortex of gestation day 17 Wistar rat embryos. The proportions of MAP2-positive cells (red) and GFAP-positive cells (green) in each experiment were estimated to be 70% and 30%, respectively (A). The cultured cells were infected with 3.0×10^{10} particles of either AAV2CMVLZ or AAV5CMVLZ per well and incubated for 72 h. Co-localization of X-gal and either MAP2- or GFAP-positive cells was examined under the fluorescence microscope. The co-localized cells was counted to estimate the transduction efficiency of rAAVs. One hundred MAP2- or GFAP-positive cells were counted and the percentage of X-gal positive cells was determined (B). The result shown is the average of five different experiments. The mean and SD for each group are presented as histograms. AAV2CMVLZ transduction to MAP2-positive cells was significantly higher ($^*P < 0.01$) than AAV5CMVLZ, and AAV5CMVLZ transduction to GFAP-positive cells was significantly higher ($^*P < 0.01$) than AAV2CMVLZ. Significant differences between AAV2CMVLZ and AAV5CMVLZ were tested using the Mann–Whitney non-parametric test.

multipolar neuronal features. A few positive cells were also detected in the pyramidal and granular cell layers. The β-galactosidase expression of AAV5CMVLZ is shown in Fig. 3B. This vector achieved a higher overall β-galactosidase expression level and had a markedly different expression pattern compared to AAV2CMVLZ. The transgene expression patterns of the rAAVs driven by the RSV promoter, which were observed dominantly in the pyramidal cell and granular cell layers, are shown in Fig. 3C,D. AAV2RSVLZ achieved a much higher expression in the pyramidal cell layer than AAV5RSVLZ (Fig. 3C), while AAV5RSVLZ achieved a higher expression in the granular cell layer (Fig. 3D). The distribution of cell surface-linked α-2,3 sialic acid, a putative receptor of rAAV5, in the gerbil hippocampus was examined using Maackia amurensis lectin II (MAL II). Briefly, the sections were incubated with 10 μg/ml biotinylated MAL II (Vector Laboratories Inc.), and then consecutively incubated with fluorescent avidin conjugates (Molecular Probes, Inc. Eugene, OR). Stained sections were observed under the fluorescent microscope. The affinity of the lectin to the granular cell layer was higher than that to the CA1 pyramidal cell layer (Fig. 3E,F). Accordingly, we detected more α-2,3 sialic acid around the cells in the granular cell layer.

In this study, we examined the potential regional tropism of both the rAAV2 and rAAV5 vectors, each with either the CMV or RSV promoters, for gene delivery to primary cultured cells and the gerbil hippocampus. rAAV5 achieved a higher expression of GFAP-positive cells than rAAV2 in vitro. In the gerbil hippocampus, AAV2CMVLZ-driven transgene expression was preferentially found in the stratum oriens, while AAV5CMVLZ-driven transgene expression was found throughout the hippocampus. rAAV5 with the CMV promoter, but not the RSV promoter, enhanced the overall diffuse transgene expression. AAV2RSVLZ achieved increased expression in the pyramidal cell layer, while AAV5RSVLZ achieved increased expression in the granular cell layer. The amount of α-2,3 sialic acid, a putative rAAV5 receptor [5,17], in the granular cell layer was greater than that in the CA1 pyramidal cell layer. The CMV early promoter is one of the strongest constitutively active virus-derived transcription elements and has been used in many vector systems, including rAAV. Although there have been several reports suggesting that other promoters such as NSE, EF-1α, and PDGF-β are more suitable than the CMV promoter for transgene expression using rAAV2 [8,12,18], others have reported that the CMV promoter efficiently drives expression in astrocytes but not in neurons during adenovirus-mediated infection [15]. A previous study also revealed that rAAV5 could infect large number of cells with long-lasting expression in both neuronal and glial cells [2]. These findings are consistent with the rAAV5-mediated enhanced hippocampal expression with the CMV promoter observed in our study. A higher affinity of rAAV5 to the astrocytes than that of rAAV2 could account for the higher transgene expression level in vivo that is obtained using rAAV5 with the CMV promoter. We found that the activity of the RSV promoter was superior to the CMV promoter in achieving efficient transgene expression in the pyramidal neurons in the hippocampus. In contrast to recombinant adenovirus containing the RSV promoter, which preferentially achieves

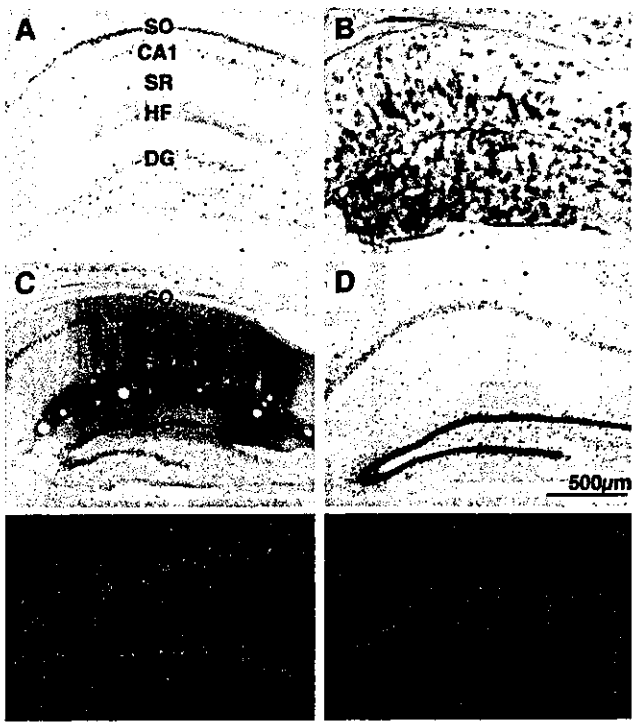

Fig. 3. Transgene expression following injection of rAAVs into the gerbil hippocampus and distribution of α-2,3 sialic acid in the gerbil hippocampus. rAAV2 and rAAV5 vectors with either the CMV or RSV promoters were injected into the gerbil hippocampus using stereotaxic apparatus. Five days after injection, transgene expression was examined by X-gal staining (A–D). Staining patterns of AAV2CMVLZ (A), AAV5CMVLZ (B), AAV2RSVLZ (C), and AAV5RSVLZ (D) are shown. Apical dendrites of pyramidal cells were visible in the stratum oriens (SO) and stratum radiatum (SR) (C). Fibers are strongly stained in the hippocampal fissure (HF) (C). The distribution of α-2,3 sialic acid was analyzed with a MAL II-binding assay. α-2,3 sialic acid was detected on the inner side of the granular cell layer, indicating the fibers arising from the granular cells (arrowheads, white signal) (E). In the CA1 pyramidal cell layer, a smaller amount of α-2,3 sialic acid was detected around the cells (F). Original magnification: 80× (A–D), 400× (E,F); DG, dentate gyrus; CA1, CA1 pyramidal cell layer.

transgene expression in granular cells and not in pyramidal cells [15], AAV2RSVLZ showed widespread and strong transgene expression in pyramidal cells. As the rAAV with the 1.8 kb NSE promoter was also reported to have enhanced transgene expression in pyramidal cells [8,18], the 0.4 kb RSV promoter has the advantage of a large transgene capacity for rAAV-mediated neuronal expression in the hippocampus. Since rAAV has a relatively small packaging capacity, the promoter length is a critical factor in determining the size limitation of the transgene [3]. A larger amount of α-2,3 sialic acid was observed in the granular cell layer than in the CA1 pyramidal cell layer, suggesting that the distribution of the AAV5 receptor on granular cells might be partially responsible for the predominant transgene expression of AAV5RSVLZ in granular cells. Specifically, AAV2RSVLZ is more suitable for driving transgene expression in the pyramidal cell layer than AAV5RSVLZ. We could successfully observe distinct transgene expression in the hippocampus using rAAVs with the proper serotypes and promoters. Using these and similar vectors, the roles of specific proteins in each brain subregion can be investigated in a simpler and faster manner. In particular, broad and efficient transgene expression in the pyramidal cell layer should prove valuable for the functional analysis of the selective ischemic neuronal death that occurs in the CA1 region. Furthermore, for elucidating the mechanism of ischemic delayed neuronal death, the results obtained here indicate that rAAV2 with the RSV promoter would be beneficial for expressing non-secretory intra-cellular proteins, while rAAV5 with the CMV promoter may be useful for the delivery of secretory proteins such as neurotrophic factors. Many other applications are also foreseeable using optimized rAAV-mediated gene transfer to the hippocampal neurons.

Acknowledgements

The authors thank Dr John A. Chiorini for providing pAAV5RNL and pAAV5RepCap (identical to 5RepCapB). We wish to thank Avigen, Inc. (Alameda, CA) for providing pAAVlacZ, pHLP19, and pAdeno. We also thank Mrs Miyoko Mitsu for her encouragement and technical support. This work was supported in part by grants from the Ministry of Health, Labour and Welfare of Japan, Grants-in-Aid for Scientific Research from the Ministry of Education, Culture, Sports, Science and Technology of Japan.

References

[1] J.A. Chiorini, F. Kim, L. Yang, R.M. Kotin, Cloning and characterization of adeno-associated virus type 5, J. Virol. 73 (1999) 1309–1319.
[2] B.L. Davidson, C.S. Stein, J.A. Heth, I. Martins, R.M. Kotin, T.A. Derksen, J. Zabner, A. Ghodsi, J.A. Chiorini, Recombinant adeno-associated virus type 2, 4, and 5 vectors: transduction of variant cell types and regions in the mammalian central nervous system, Proc. Natl. Acad. Sci. USA 97 (2000) 3428–3432.
[3] J.Y. Dong, P.D. Fan, R.A. Frizzell, Quantitative analysis of the packaging capacity of recombinant adeno-associated virus, Hum. Gene Ther. 7 (1996) 2101–2112.
[4] D. Duan, Z. Yan, Y. Yue, W. Ding, J.F. Engelhardt, Enhancement of muscle gene delivery with pseudotyped adeno-associated virus type 5 correlates with myoblast differentiation, J. Virol. 75 (2001) 7662–7671.
[5] N. Kaludov, K.E. Brown, R.W. Walters, J. Zabner, J.A. Chiorini, Adeno-associated virus serotype 4 (AAV4) and AAV5 both require sialic acid binding for hemagglutination and efficient transduction but differ in sialic acid linkage specificity, J. Virol. 75 (2001) 6884–6893.
[6] R.P. Kesner, P.E. Gilbert, G.V. Wallenstein, Testing neural network models of memory with behavioral experiments, Curr. Opin. Neurobiol. 10 (2000) 260–265.
[7] T. Kirino, Delayed neuronal death in the gerbil hippocampus following ischemia, Brain Res. 239 (1982) 57–69.
[8] R.L. Klein, E.M. Meyer, A.L. Peel, S. Zolotukhin, C. Meyers, N. Muzyczka, M.A. King, Neuron-specific transduction in the rat

septohippocampal or nigrostriatal pathway by recombinant adeno-associated virus vectors, Exp. Neurol. 150 (1998) 183–194.
[9] M.Y. Mastakov, K. Baer, R.M. Kotin, M.J. During, Recombinant adeno-associated virus serotypes 2- and 5-mediated gene transfer in the mammalian brain: quantitative analysis of heparin co-infusion, Mol. Ther. 5 (2002) 371–380.
[10] T. Matsushita, S. Elliger, C. Elliger, G. Podsakoff, L. Villarreal, G.J. Kurtzman, Y. Iwaki, P. Colosi, Adeno-associated virus vectors can be efficiently produced without helper virus, Gene Ther. 5 (1998) 938–945.
[11] T. Okada, H. Mizukami, M. Urabe, T. Nomoto, T. Matsushita, Y. Hanazono, A. Kume, K. Tobita, K. Ozawa, Development and characterization of an antisense-mediated prepackaging cell line for adeno-associated virus vector production, Biochem. Biophys. Res. Commun. 288 (2001) 62–628.
[12] J.C. Paterna, T. Moccetti, A. Mura, J. Feldon, H. Bueler, Influence of promoter and WHV post-transcriptional regulatory element on AAV-mediated transgene expression in the rat brain, Gene Ther. 7 (2000) 1304–1311.
[13] W.A. Pulsinelli, J.B. Brierley, F. Plum, Temporal profile of neuronal damage in a model of transient forebrain ischemia, Ann. Neurol. 11 (1982) 491–498.
[14] Y. Shen, S.I. Muramatsu, K. Ikeguchi, K.I. Fujimoto, D.S. Fan, M. Ogawa, H. Mizukami, M. Urabe, A. Kume, I. Nagatsu, F. Urano, T. Suzuki, H. Ichinose, T. Nagatsu, J. Monahan, I. Nakano, K. Ozawa, Triple transduction with adeno-associated virus vectors expressing tyrosine hydroxylase, aromatic-L-amino-acid decarboxylase, and GTP cyclohydrolase I for gene therapy of Parkinson's disease, Hum. Gene Ther. 11 (2000) 1509–1519.
[15] A.F. Shering, D. Bain, K. Stewart, A.L. Epstein, M.G. Castro, G.W. Wilkinson, P.R. Lowenstein, Cell type-specific expression in brain cell cultures from a short human cytomegalovirus major immediate early promoter depends on whether it is inserted into herpesvirus or adenovirus vectors, J. Gen. Virol. 78 (1997) 445–459.
[16] K. Shimazaki, M. Urabe, J. Monahan, K. Ozawa, N. Kawai, Adeno-associated virus vector-mediated bcl-2 gene transfer into post-ischemic gerbil brain in vivo: prospects for gene therapy of ischemia-induced neuronal death, Gene Ther. 7 (2000) 1244–1249.
[17] R.W. Walters, S.M. Yi, S. Keshavjee, K.E. Brown, M.J. Welsh, J.A. Chiorini, J. Zabner, Binding of adeno-associated virus type 5 to 2,3-linked sialic acid is required for gene transfer, J. Biol. Chem. 276 (2001) 20610–20616.
[18] R. Xu, C.G. Janson, M. Mastakov, P. Lawlor, D. Young, A. Mouravlev, H. Fitzsimons, K.L. Choi, H. Ma, M. Dragunow, P. Leone, Q. Chen, B. Dicker, M.J. During, Quantitative comparison of expression with adeno-associated virus (AAV-2) brain-specific gene cassettes, Gene Ther. 8 (2001) 1323–1332.
[19] J. Zabner, M. Seiler, R. Walters, R.M. Kotin, W. Fulgeras, B.L. Davidson, J.A. Chiorini, Adeno-associated virus type 5 (AAV5) but not AAV2 binds to the apical surfaces of airway epithelia and facilitates gene transfer, J. Virol. 74 (2000) 3852–3858.

Gene Therapy (2003) 10, 375–385

www.nature.com/gt

RESEARCH ARTICLE

Enhancement of thymidine kinase-mediated killing of malignant glioma by BimS, a BH3-only cell death activator

T Yamaguchi[1], T Okada[2], K Takeuchi[3], T Tonda[4], M Ohtaki[4], S Shinoda[1], T Masuzawa[1], K Ozawa[2] and T Inaba[5]

[1]*Department of Surgical Neurology, Center of Molecular Medicine, Jichi Medical School, Tochigi, Japan;* [2]*Division of Genetic Therapeutics, Center of Molecular Medicine, Jichi Medical School, Tochigi, Japan;* [3]*Department of Anatomy, Center of Molecular Medicine, Jichi Medical School, Tochigi, Japan;* [4]*Department of Environmetrics and Biometrics, Research Institute for Radiation Biology and Medicine, Hiroshima University, Hiroshima, Japan; and* [5]*Department of Molecular Oncology, Research Institute for Radiation Biology and Medicine, Hiroshima University, Hiroshima, Japan*

Herpes simplex virus thymidine kinase (HSV-tk)/gancyclovir (GCV) therapy has the ability to inhibit tumor formation in animal models but the results of clinical trials have been disappointing. To improve the performance of tk/GCV therapy, we tried combination therapy designed to enhance its cytotoxic effects by introducing genes that induce apoptosis of the tumor cells through different pathways. We concentrated our efforts on the use of Bim, a BH3-only member of death activators in the Bcl-2 superfamily, because Bim is not involved in the pathways through which HSV-tk/GCV therapy induces apoptosis in malignant glioma cells. Among three alternative splicing variants, BimEL, BimL, and BimS, BimS lacks the binding domain for the dynein light chain LC8, which negatively regulates the proapoptotic function of BimEL and BimL. All four malignant glioma cell lines, U251, A172, T-430, and U373 underwent cell death after transfer of BimS using an adenovirus vector (AVC2). Intriguingly, combination of AVC2-BimS with AVC2-tk markedly increased the sensitivity of U251 cells to GCV both in vitro and in vivo. In contrast, AVC2-BimL did not induce significant cell death. These results indicated that BimS had the ability to improve the efficiency of HSV-tk/GCV therapy in the treatment of malignant glioma and suggested that the targeting of different proapoptotic pathways may be a useful strategy for the development of an effective gene therapy approach to treatment.
Gene Therapy (2003) **10,** 375–385. doi:10.1038/sj.gt.3301897

Keywords: *tk/GCV therapy; malignant glioma; Bim; apoptosis; adenovirus*

Introduction

Since conventional treatments for malignant glioma have made little progress during the last several decades, the development of new therapeutic approaches has been the focus of intensive research. One such approach, herpes simplex virus thymidine kinase (HSV-tk)/gancyclovir (GCV) enzyme-prodrug therapy has shown the most promise and has several advantages.[1,2] First, neurons are not damaged by this treatment because, when using retrovirus vectors, the HSV-*tk* gene is only transferred into dividing cells; thus, such treatment only targets proliferating cells. Second, tumor cells without HSV-*tk* gene transduction can be killed through the bystander effect by a mechanism that is not fully understood.[3] Results of clinical trials of HSV-tk/GCV therapy, however, have been disappointing.[4,5] Thus, we attempted to develop a strategy that would improve the performance of HSV-tk/GCV therapy when applied in combination.

Correspondence: Dr T Inaba, Department of Molecular Oncology, Research Institute for Radiation Biology and Medicine, Hiroshima University, 1-2-3 Kasumi, Minami-ku, Hiroshima 734-8553, Japan
Received 14 April 2002; accepted 6 August 2002

Our approach derived its rationale from recent progress that was made in understanding the mechanisms through which members of the Bcl-2 superfamily regulate apoptosis. The expression or function of each member of this superfamily is known to be regulated in response to specific death triggers. For example, in hematopoietic cells, an antiapoptotic member, Bcl-x_L, is downregulated by cytokine withdrawal through inactivation of JAK-STAT pathways,[6–10] while DNA damage induced by ionizing radiation (IR) usually does not alter its expression levels.[11] In contrast, IR induces a proapoptotic member, Bax, by activating p53-dependent pathways,[12] while cytokine withdrawal does not.[7] The regulation of Bcl-x_L and Bax through distinct pathways in hematopoietic cells might be conserved in glioma cells. Indeed, insulin-like growth factor I regulates the expression of Bcl-x_L but not Bax,[13] which is induced in cells undergoing apoptosis as a result of DNA damage induced by IR or HSV-tk/GCV treatment.[14,15] Because members of the Bcl-2 superfamily on the outer membrane of mitochondria integrate signals affecting cell fate and ultimately control the translocation of cytochrome *c* and other apoptosis-initiating proteins from the mitochondria to the cytosol,[16] enforced expression of different Bcl-2 superfamily members other than those induced

by HSV-tk/GCV therapy might efficiently enhance its cytotoxic effects.

We and others recently established that the expression and/or function of Bim, a BH3-only member of death activators in the Bcl-2 superfamily, is upregulated by cytokine withdrawal through the inactivation of Ras-phosphatidylinositol 3-kinase (PI3-K) pathways but not by DNA damage induced by IR in hematopoietic cells.[11,17] It was also reported that Bim was induced in sympathetic neurons undergoing apoptosis that was triggered by the removal of neurotrophic factors.[18,19] Thus, we speculated that Bim might be a candidate for enhancing the cytotoxic effect of HSV-tk/GCV on malignant glioma cells through different proapoptotic pathways. Bim was isolated independently by two groups that exploited its ability to bind Bcl-2 and Mcl1.[20,21] Alternative splicing of Bim gives rise to three variants, BimEL, BimL, and BimS, each of which contains the BH3 domain and functions as a death inducer. In certain cell types, BimEL and BimL, but not BimS, bind to M_r=8000 dynein light chain, LC8 (also PIN or Dlc-1),[22,23] which negatively regulates the proapoptotic function of the former two isoforms.[24]

In this study, we introduced the *Bim* genes into glioma cells *in vitro* and *in vivo* using adenovirus vectors. BimS but not BimL efficiently induced apoptosis in glioma cells. Moreover, BimS markedly enhanced the cytotoxic effects of HSV-tk/GCV therapy.

Results

Expression of the Bcl-2 superfamily members in human malignant glioma cell lines

Our basic strategy to improve the performance of HSV-tk/GCV therapy was to induce apoptosis in glioma cells through different cell death pathways. To test whether Bim was a good candidate, we analyzed protein expression in cell lines established from human malignant gliomas, as well as an HL60 human leukemia cell line as a positive control (Figure 1a, lane 1). Immunoblot analyses using antibodies specific for the Bcl-2 superfamily members revealed expression of Bcl-x_L and Bim in glioma cells, while Bcl-2 protein was barely detectable (lanes 2–6). To identify genes that specifically responded to HSV-tk/GCV therapy, U251 cells were infected with AVC2-tk and were treated with 10 μM GCV after 48 h. Expression of Bax was induced as previously reported by others,[15] while expression levels of Bim were not altered (Figure 1b). These data suggested that the enforced expression of Bim may efficiently enhance the cytotoxic effects of HSV-tk/GCV therapy.

In vitro transfer of Bim genes to U251 malignant glioma cells using adenovirus vectors

In this study, we employed adenovirus vectors, which showed uniformly high infection efficiency in malignant glioma cells (data not shown). When using wild-type 293 cells for virus amplification at an MOI of 0.001, we obtained low-titer virus stocks around 1×10^9 pfu/ml for AVC2-BimS and AVC2-BimL, which was less than one thousandth of that for AVC2-tk, because 293 cells were killed within 24 h of infection (data not shown). By using 293B cells, which stably overexpressed Bcl-x_L protein (see Materials and methods), the titer of AVC2-BimS and AVC2-BimL stock was improved to 1×10^{11} and 2.5×10^{11} pfu/ml, respectively, at the same MOI.

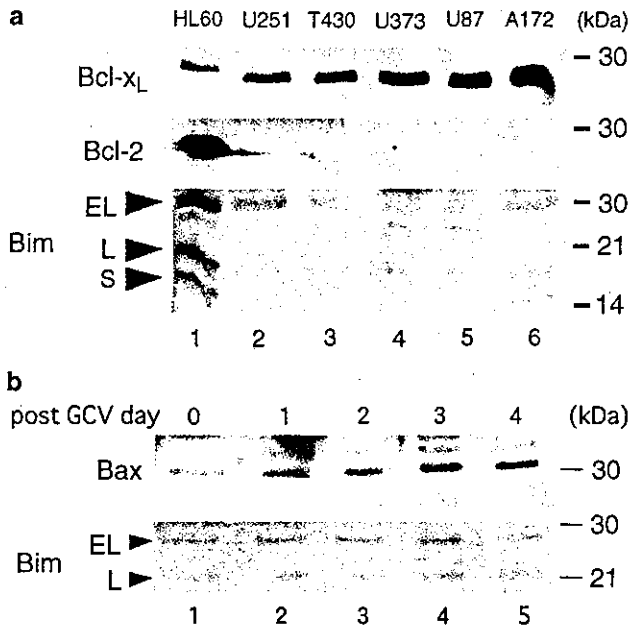

Figure 1 Immunoblot analysis of the Bcl-2 superfamily members in malignant glioma cell lines. (a) Cell extracts from HL-60 (positive control, lane 1), U251 (lane 2), T430 (lane 3), U373 (lane 4), U87 (lane 5), and A172 (lane 6) cells were subjected to immunoblot analysis using antibodies for Bcl-x (top panel), Bcl-2 (middle panel), and Bim (bottom panel). (b) U251 cells were infected with AVC2-tk at an MOI of 20 and GCV was added to the culture medium at a concentration of 10 mM, 48 h after infection. Cells remained in culture for the number of days indicated above. Bax (top panel) and Bim (bottom panel) proteins were detected using antibodies specific for each protein.

When U251 glioma cells were infected by AVC2-BimL or -BimS at an MOI of 20, most of the cells were GFP-positive (Figure 2a) and expressed Bim proteins at high levels (Figure 2b) within 24 h of infection. Endogenously expressed Bim protein in U251 cells (Figure 1a, lane 2) was barely detectable in Figure 2b because of short exposure time. Cells infected by AVC2-BimS appeared shrunken and were fragmented (Figure 2a, left panel). Indeed, approximately 80% of these cells were positive for apoptosis using the TUNEL assay (Figure 3b) and had typical apoptotic changes including shrunken nuclei with perinuclear chromatin condensation, loss of pseudopods, and preservation of cytoplasmic organelles as shown by electron microscopy (Figure 4), indicating that BimS efficiently induced apoptosis in U251 cells. In contrast, cells infected by AVC2-BimL looked healthy (Figure 2a, right panel), and were negative for apoptosis using the TUNEL assay (Figure 3d), despite their high-level expression of BimL protein (Figure 2b). Control cells that were infected by AVC2-tk without GCV treatment were also negative for TUNEL analysis (Figure 3f). These results suggested that the proapoptotic function of BimL was downregulated through the binding of LC8 and also that apoptosis induced by the AVC2-BimS was preferentially caused by BimS protein, rather than being due to nonspecific toxicity of the adenovirus. Rapid cell death induced by BimS but not by BimL was observed in other glioma cell lines including A172, T-430 and U373 (data not shown).

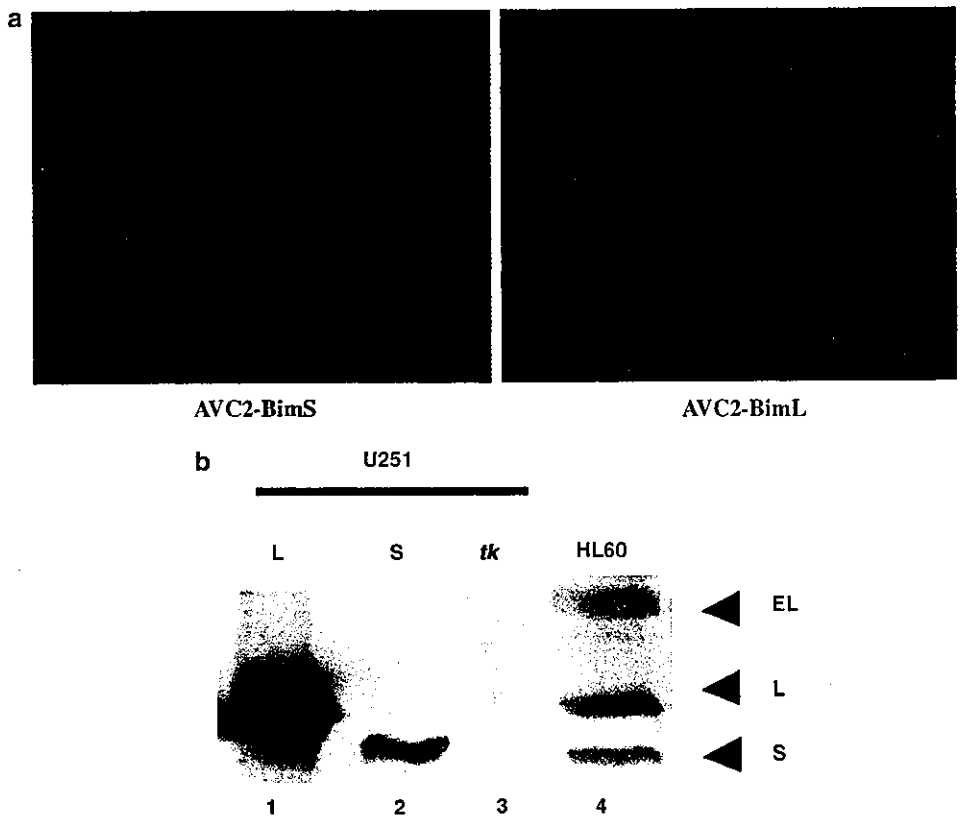

Figure 2 Expression of GFP and Bim proteins. (a) GFP expression was detected in U251 cells that received AVC2-BimS (left panel) or AVC2-BimL (right panel), using fluorescence microscopy 24 h after infection. (b) Bim proteins were detected by immunoblot analysis of cell extracts from U251 cells infected by AVC2-BimL (lane 1), AVC2-BimS (lane 2), or AVC2-tk (lane 3) after 24 h, as well as from control, HL-60 cells (lane 4).

Enhancement of cytotoxic effects of HSV-tk/GCV treatment by BimS in vitro

We evaluated the cytotoxic effects of Bim proteins and their capacity to enhance HSV-tk/GCV treatment using the XTT assay. U251 cells were infected with AVC2-BimS, AVC2-BimL, or AVC2-tk at relatively high MOIs and XTT assay was performed after 3 days (Figure 5a). AVC2-BimS showed MOI-dependent cytotoxicity potential, while AVC2-BimL and AVC2-tk without GCV treatment (tk/PBS) had no cytotoxic effect at MOIs below 100. AVC2-tk followed by GCV treatment (tk/GCV) showed no effect at this time point, implicating BimS in the mediation of this rapid cytotoxic effect.

Next, we infected U251 cells with AVC2-BimS or AVC2-BimL as the sole adenovirus vector or in combination with AVC2-tk at relatively low MOIs and tested cytotoxicity on day 7 (Figure 5b). Neither AVC2-BimL, tk/PBS, nor the combination of these treatments showed cytotoxicity. However, AVC2-BimS, tk/GCV, and combinations containing either of these two treatments (ie, combination of AVC2-BimS and tk/PBS, and combination of AVC2-BimL and tk/GCV) had cytotoxic effects at an MOI of 25. Intriguingly, cytotoxic potential obtained by the combination of tk/GCV and BimS (tk/GCV+BimS) treatment seemed to be higher than that obtained by an additive effect of tk/GCV and BimS. For testing statistical significance of joint effect of tk/GCV and BimS, a likelihood ratio test was conducted in the following ways. Let y_{ij} (j=1,...,8; i=1,2,3) be the response variable at the jth MOI level for the ith treatment, where i=1,2, and 3 means the treatment with BimS, tk/GCV, and tk/GCV+BimS, respectively. Then we consider the Weibull curve model

$$y_{ij} = \exp\{-(d_j/\mu_i)^{\alpha_i}\} + \epsilon_{ij},$$

where ϵ_{ij} is the error term, and μ_i, and α_i are unknown positive parameters. By transforming y_{ij} to

$$z_{ij} = \zeta \log\{-(\log y_{ij} - \xi)\},$$

we induced the following simple linear model,

$$z_{ij} = \beta_{i0} + \beta_{i1} \log d_j + e_{ij}, e_{ij} \sim N(0, \sigma^2)\},$$

where ζ is the constant for adjustment such that total variance of z_{ij} is unity, and ξ is the constant for each response being common at d_j=0. The null hypothesis was formulated as H_0:β_{3k}=β_{1k}+β_{2k} (k=0,1), where there exists no joint effect of 'tk/GCV+BimS'. Let L be the likelihood with no restriction and L_0 be one under H_0. Then the likelihood ratio test statistic T=−2log(L_0/L) is asymptotically distributed as Chi-squared distribution having the numbers of restricted parameters as its degree of freedom. The result shows that H_0 is rejected with a high significance level of $P<0.01$, which means that the joint effect of tk/GCV and BimS can be expected more than the independent multiplier one (Figure 5c). Similar results were observed in U373 and T-430 cells (Figures 5d and e).